iScience

CellPress
OPEN ACCESS

Review

# The glymphatic system: Current understanding and modeling

Tomas Bohr,[1] Poul G. Hjorth,[2] Sebastian C. Holst,[3] Sabina Hrabětová,[4] Vesa Kiviniemi,[5,6] Tuomas Lilius,[7,8,9,10] Iben Lundgaard,[11,12] Kent-Andre Mardal,[13,14] Erik A. Martens,[15] Yuki Mori,[16] U. Valentin Nägerl,[17] Charles Nicholson,[18,19] Allen Tannenbaum,[20] John H. Thomas,[21] Jeffrey Tithof,[22] Helene Benveniste,[23,24] Jeffrey J. Iliff,[25,26,27] Douglas H. Kelley,[21,30,*] and Maiken Nedergaard[28,29,*]

## SUMMARY

**We review theoretical and numerical models of the glymphatic system, which circulates cerebrospinal fluid and interstitial fluid around the brain, facilitating solute transport. Models enable hypothesis development and predictions of transport, with clinical applications including drug delivery, stroke, cardiac arrest, and neurodegenerative disorders like Alzheimer's disease. We sort existing models into broad categories by anatomical function: Perivascular flow, transport in brain parenchyma, interfaces to perivascular spaces, efflux routes, and links to neuronal activity. Needs and opportunities for future work are highlighted wherever possible; new models, expanded models, and novel experiments to inform models could all have tremendous value for advancing the field.**

## PREFACE

The authors of this paper came together in October 2021 for a workshop entitled "The glymphatic system: From theoretical models to clinical applications." As the title suggests, although experiments were a common topic of discussion, our primary focus was modeling: Reconciling observations with theory to construct a broad conception of the flow of cerebrospinal fluid in the brain, along with its clinical implications. We not only shared recent research results but also engaged in extended, moderated conversations among all participants, seeking to identify topics of broad consensus in the field, topics of controversy, and future work that could settle controversies, thereby producing key knowledge to advance the field. The purpose of this article is to summarize the shared understanding we developed.

Accordingly, this article is not a broad review of cerebrospinal fluid flow in the brain or central nervous system. (We direct readers to other recent publications for excellent reviews of the glymphatic system (Rasmussen et al., 2021; Benveniste et al., 2019b; Nedergaard and Goldman, 2020; Ray and Heys, 2019; Linninger et al., 2016) and alternate perspectives on cerebrospinal fluid flow in the brain (Hladky and Barrand, 2022; Tarasoff-Conway et al., 2016; Engelhardt et al., 2016).) Rather, we focus on theoretical and mathematical modeling of the glymphatic system, especially where it might benefit clinicians and experimentalists, while also noting where future experiments are needed for improved models. It is increasingly clear that the glymphatic system, rightfully understood for the last decade as being capable of clearing brain metabolic waste, also does much more and is a fundamental facet of neurobiology. Because it seems to play an essential clinical role for degenerative disorders such as Alzheimer's disease (Nedergaard and Goldman, 2020), stroke (Mestre et al., 2020a), and cardiac arrest (Du et al., 2022), and because of the potential as a novel route for drug delivery (Plog et al., 2018; Lilius et al., 2019), interest is growing exponentially, and new modelers are joining the field in large numbers. If you are among them, we welcome you and hope this article will prove useful. If you are an established expert, we hope that you will nonetheless find insight and a coherent vision in this article. Throughout, we have made every effort to delineate where evidence leads to broad consensus, where uncertainties leave room for current controversies, and what future work could resolve old questions and make way for new ones. For further information, we refer you to another recent, and excellent, review of glymphatic modeling (Martinac and Bilston, 2019).

The article proceeds as follows. Rapid review presents a rapid review, limited to topics necessary for the subsequent discussion, noting topics of consensus and controversy. Mechanisms continues by tabulating

[1]Department of Physics, Technical University of Denmark, 2800 Kgs. Lyngby, Denmark

[2]Department of Applied Mathematics and Computer Science, Technical University of Denmark, Richard Petersens Plads, 2800 Kgs. Lyngby, Denmark

[3]Neuroscience and Rare Diseases Discovery and Translational Area, Roche Pharmaceutical Research and Early Development, Roche Innovation Center Basel, Grenzacherstrasse 124, 4070 Basel, Switzerland

[4]Department of Cell Biology and The Robert Furchgott Center for Neural and Behavioral Science, State University of New York Downstate Medical Center, Brooklyn, NY, USA

[5]Oulu Functional NeuroImaging, Department of Diagnostic Radiology, MRC, Oulu University Hospital, Oulu, Finland

[6]Medical Imaging, Physics and Technology, the Faculty of Medicine, University of Oulu, Oulu, Finland

[7]Department of Pharmacology, Faculty of Medicine, University of Helsinki, Helsinki, Finland

[8]Individualized Drug Therapy Research Program, Faculty of Medicine, University of Helsinki, Helsinki, Finland

[9]Center for Translational Neuromedicine, Faculty of Health and Medical Sciences, University of Copenhagen, Copenhagen, Denmark

[10]Department of Emergency Medicine and Services, Helsinki University Hospital and University of Helsinki, Helsinki, Finland

*Continued*

known and proposed mechanisms of fluid flow and solute transport in the brain, with links to neuronal activity. Modeling discusses theoretical models devised for each mechanism discussed in the prior section, and also gives an introduction to optimal mass transport, a powerful method for inferring *in vivo* flows in order to test theoretical models. Section Use case: Drug delivery presents one use case in which glymphatic models could have concrete impact in the near future: drug delivery. Finally, Use case: Drug delivery considers the outlook for glymphatic modeling and proposes future work to move the field forward.

## RAPID REVIEW

### The glymphatic model, past and present

#### *The initial description of the glymphatic system*

Throughout the body, the extracellular space is essential for cell-cell signaling, as well as the import and distribution of metabolic substrates and the export of waste. In the periphery, a steady influx of plasma ultrafiltrate drives interstitial fluid (ISF) into tissues, whereas excess fluid and metabolic waste products are exported by lymphatic vessels (Wiig and Swartz, 2012; Moore and Bertram, 2018). Fluid transport in the central nervous system (CNS) differs from peripheral tissue, first by the presence of the blood-brain barrier (BBB) that restricts fluid and solute exchange with the vascular compartment, and second by the absence of lymphatic vessels from neural tissue. It is therefore no surprise that diffusion processes traditionally are regarded as primarily responsible for solute distribution in the CNS (Abbott, 2004; Syková and Nicholson, 2008).

In a series of four studies published in 2012–2013, the anatomical organization, function, and physiological regulation of the "glymphatic" system was first described using dynamic imaging techniques. In the initial study (Iliff et al., 2012), *in vivo* two-photon microscopy was used to characterize the rapid unidirectional influx of cerebrospinal fluid (CSF) into and through brain tissue along perivascular spaces surrounding cerebral arteries. Interstitial solutes, in turn, were cleared from the brain along white matter tracts and large draining veins towards cisternal CSF compartments associated with dural venous sinuses. Both perivascular CSF influx and interstitial solute clearance, including that of amyloid beta, were sensitive to the deletion of the gene encoding the astroglial water channel aquaporin-4 (AQP4), demonstrating that glymphatic function is dependent on astroglial water transport. A subsequent *in vivo* two-photon microscopy study showed that cerebral arterial pulsation was a key driver of this perivascular exchange (Iliff et al., 2013a), whereas a study utilizing dynamic contrast-enhanced magnetic resonance imaging (DCE-MRI) documented that glymphatic exchange occurs throughout the brain and is organized macroscopically along the scaffold of the cerebral arterial vasculature (Iliff et al., 2013b). The final study of this sequence showed that perivascular CSF influx and interstitial solute efflux, including the clearance of amyloid beta, are more rapid in the sleeping compared to the waking brain (Xie et al., 2013).

Although these initial studies framed the present understanding of glymphatic function, it is important to note that several aspects of brain fluid transport had already been shown. Periarterial CSF influx and perivenous interstitial solute efflux were clearly described by Rennels et al. in studies that identified arterial pulsation as the key driver of perivascular exchange (Rennels et al., 1985, 1990). Yet, these findings were quickly rejected as an artifact of the histological procedure by their contemporaries (Abbott, 2004; Ichimura et al., 1991). Interest faded, in part because other groups could not replicate the original findings, but also because no function for perivascular flow was proposed. The novelty of the glymphatic concept stemmed from the integration of CNS perivascular exchange with clearance of amyloid beta, dependence on AQP4, and sleep-wake regulation within a single physiological framework. Another important aspect of the glymphatic studies was that they were critically enabled by the development of imaging techniques including two-photon microscopy and DCE-MRI, which permitted the processes of fluid and solute exchange to be visualized in real-time, non-invasively (without opening the skull or disrupting the meninges), and in the living brain. Indeed, it is the use of MRI that has enabled the validation of these initial findings in rodents in the primate (Goulay et al., 2017) and human brain (Ringstad et al., 2017; Eide et al., 2021c).

#### *An evolving understanding of glymphatic biology*

Based on these initial studies, the "glymphatic" system was named based on its dependence on perivascular AQP4 astroglial water channels and its similarities in function to the peripheral lymphatic system.

The initial description of the glymphatic system focused on advective periarterial CSF influx, perivenous interstitial solute efflux, and a dependence on astroglial water transport. By now, more than 1000 papers

[11]Department of Experimental Medical Science, Lund University, Lund, Sweden

[12]Wallenberg Centre for Molecular Medicine, Lund University, Lund, Sweden

[13]Department of Mathematics, University of Oslo, Oslo, Norway

[14]Simula Research Laboratory, Department of Numerical Analysis and Scientific Computing, Oslo, Norway

[15]Centre for Mathematical Sciences, Lund University, Sweden

[16]Center for Translational Neuromedicine, Faculty of Health and Medical Sciences, University of Copenhagen, Copenhagen, Denmark

[17]Institut Interdisciplinaire de Neurosciences, Université de Bordeaux / CNRS UMR 5297, Centre Broca Nouvelle-Aquitaine, 146 rue Léo Saignat, CS 61292 Case 130, 33076 Bordeaux Cedex France

[18]Department of Neuroscience and Physiology, New York University Grossman School of Medicine, New York, NY, USA

[19]Department of Cell Biology, SUNY Downstate Health Sciences University, Brooklyn, NY, USA

[20]Departments of Computer Science/ Applied Mathematics and Statistics, Stony Brook University, Stony Brook, NY, USA

[21]Department of Mechanical Engineering, University of Rochester, Rochester, 14627 NY, USA

[22]Department of Mechanical Engineering, University of Minnesota, Minneapolis, USA

[23]Department of Anesthesiology, Yale School of Medicine, New Haven, CT, USA

[24]Department of Biomedical Engineering, Yale School of Medicine, New Haven, CT, USA

[25]VISN 20 Mental Illness Research, Education and Clinical Center, VA Puget Sound Health Care System, Seattle, WA, USA

[26]Department of Psychiatry and Behavioral Sciences, University of Washington School of Medicine, Seattle, WA, USA

*Continued*

have been published on the glymphatic system, and the field is rapidly expanding. The simple model proposed in 2012 remains the cornerstone depicting glymphatic export of amyloid beta on a microscopic scale, but additional twists and refinements have been added to our understanding of how fluid transport contributes to export of waste from the metabolically active brain.

In Figure 1, we provide an updated glymphatic model in which insights collected over the past nine years have been incorporated. The most important novel aspect is that the Kipnis and Alitalo groups documented the presence and function of lymphatic vessels in the meninges surrounding the brain in 2015 (Aspelund et al., 2015; Louveau et al., 2015); more were found later (Ahn et al., 2019). Intriguingly, the initial segments of the meningeal lymphatic capillaries are in close proximity to the dural venous sinuses, towards which interstitial solutes are cleared along glymphatic perivenous pathways (Rustenhoven et al., 2021). We now understand that the glymphatic system comprises the first three segments of brain fluid transport, including periarterial CSF influx, interstitial solute movement, and efflux along the perivenous spaces and cranial and spinal nerves. Lymphatic uptake and drainage represents the fourth and final step in the clearance of brain interstitial solutes from the cranium. Another key perspective that has emerged since the initial description of the glymphatic system is that while this biology is dependent on microscopic features, such as perivascular spaces, astroglial endfeet, and meningeal lymphatic vessels, it functions at the macroscopic scale of the cranium, cerebrovascular network, CSF circulation, brain and spinal cord (Figure 1). A clear understanding of its function requires consideration of the large anatomical distances that solutes must traverse within the mammalian (and particularly the human) brain, CSF dynamics throughout the ventricular, cisternal and subarachnoid compartments, the organization of the cerebrovascular tree, including both arterial segments and venous drainage, and the manner in which intracranial pressure dynamics contribute to patterns of fluid and solute movement both within fluid-filled compartments, and through the neuropil itself.

## Glymphatic function and dysfunction

### *Biological functions of the glymphatic system*

Although it has been described predominantly as "the brain's waste clearance system", the role of the glymphatic system in brain function extends beyond waste clearance alone. At a fundamental level, glymphatic function is understood to facilitate the exchange of fluid and solutes between the CSF and brain interstitial compartments — organized along perivascular pathways, driven by arterial pulsation and slow vasomotion, facilitated by astroglial water transport. For metabolic wastes, macromolecules and cellular debris that is not cleared by local cellular degradation or BBB transport, clearance to the CSF via glymphatic exchange and hence to the blood through lymphatic vessels reflects the principal route for elimination from the CNS. To date, no comprehensive study to define all of the solutes cleared from the CNS by the glymphatic system has been conducted. The select endogenous solutes that have been shown to be cleared by glymphatic transport include potassium (Monai et al., 2019); lactate; pathogenic peptides and proteins, including amyloid beta and tau; and soluble proteins released from damaged cells, including neuron-specific enolase and glial fibrillary acidic protein. In addition, such clearance contributes to CNS immune surveillance as perivascular exchange of soluble CNS antigens and interaction with associated peripheral immune cells (Rustenhoven et al., 2021; Plog et al., 2015; Lundgaard et al., 2017; Rasmussen et al., 2018).

In seminal work on choroid plexus function, Cserr proposed that both bulk flow and diffusion are necessary within the CNS to equilibrate solute concentrations between sources within the neuropil and the sink of the CSF, and prevent the formation of concentration gradients incompatible with neural function (Cserr, 1971). Although in the case of metabolic wastes this process can be thought of as "waste clearance", the same process underlies the distribution of solutes from areas of local production or entry to more distant locations. Thus, glymphatic function likely contributes to such diverse processes as volume transmission by neuromodulators, growth factor distribution, and the distribution and clearance of inflammatory cytokines (Hablitz and Nedergaard, 2021). For molecules that enter the CNS primarily across the blood-CSF barrier at the choroid plexus or are produced by the choroid plexus, such as folate and apolipoprotein E, perivascular transport supports their distribution throughout the CNS (Achariyar et al., 2016).

### *Implications for the sleep-wake regulation of glymphatic function*

A frequently overlooked element of glymphatic biology is the observation that perivascular exchange is a physiologically regulated process, and thus is not constant across different experimental conditions.

[27]Department of Neurology, University of Washington School of Medicine, Seattle, WA, USA

[28]Center for Translational Neuromedicine, Faculty of Health and Medical Sciences, University of Copenhagen, Copenhagen, Denmark

[29]Center for Translational Neuromedicine, University of Rochester Medical Center, Rochester, 14642 NY, USA

[30]Lead contact

*Correspondence: d.h.kelley@rochester.edu (D.H.K.), maiken_nedergaard@urmc.rochester.edu (M.N.)

https://doi.org/10.1016/j.isci.2022.104987

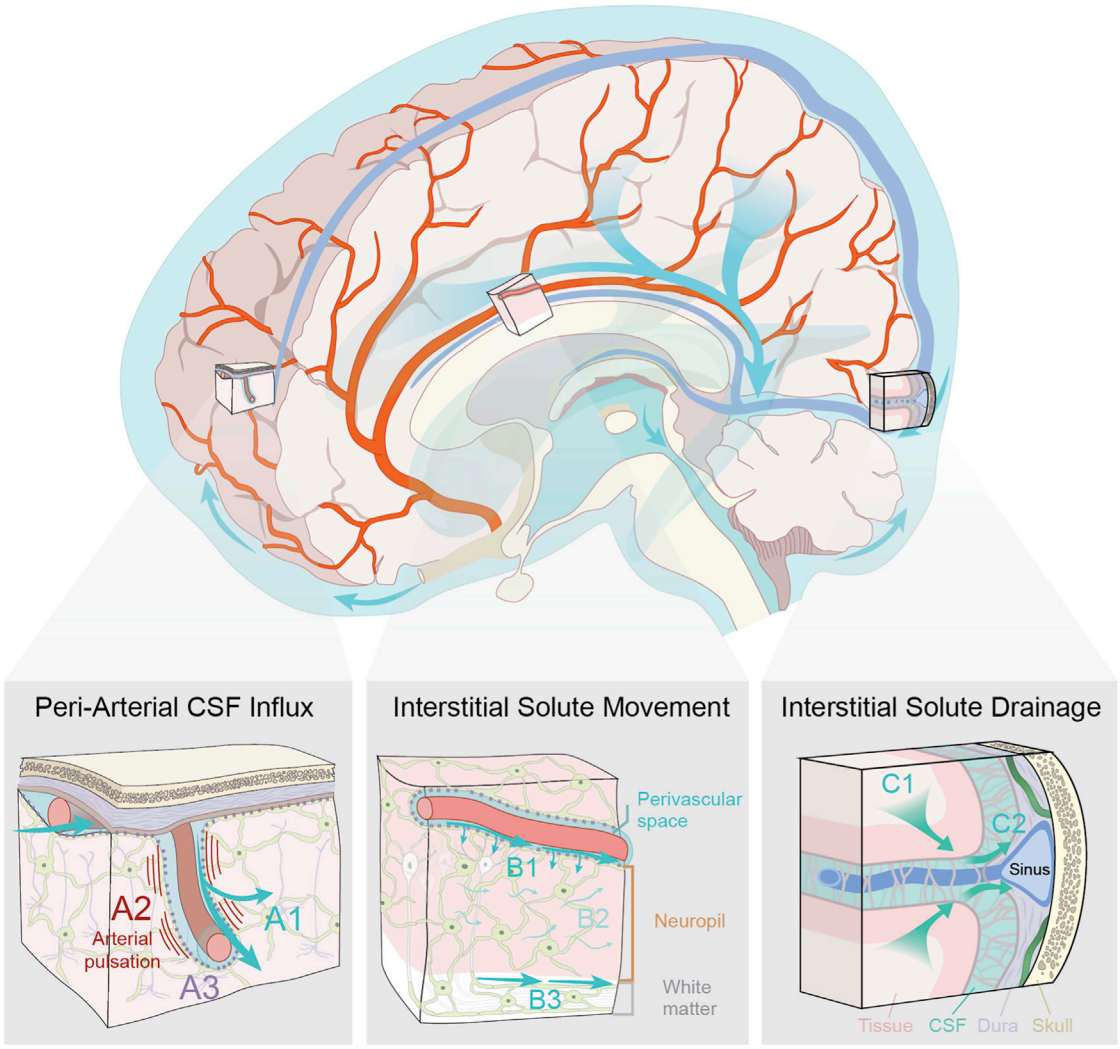


**Figure 1. Updated schematic description of the glymphatic system (2022)**

The glymphatic system supports the perivascular exchange of CSF and interstitial solutes throughout the CNS. This process occurs over macroscopic anatomical scales, within the perivascular influx of subarachnoid CSF into brain tissue organized along the scaffold of the arterial vascular network, and the efflux of interstitial solutes occurring toward cisternal CSF compartments associated with dural sinuses.

(A) CSF influx into brain tissue occurs along perivascular pathway surrounding penetrating arteries (A1) and is driven in part by arterial pulsation (A2). Perivascular bulk flow and interstitial solute clearance are dependent upon the astroglial water channel AQP4 localized to perivascular astroglial endfeet surrounding the cerebral vasculature (A3).

(B) Interstitial solute movement occurs through the combined effects of diffusion and advection. Advection is most rapid along privileged anatomical pathways, including intraparenchymal perivascular spaces (B1) and white matter tracts (B3), and supports the movement of large molecular weight solutes. Diffusion dominates the movement of small molecules, particularly within the wider interstitium (B2).

(C) Interstitial solutes drain from the parenchyma along white matter tracts and draining veins towards sinus-associated cisternal CSF compartments (C1). CSF solutes are cleared from the cranium via uptake into meningeal lymphatic vessels, by efflux through dural arachnoid granulations, or through clearance along cranial or spinal nerve sheathes (C2).

Perivascular CSF influx and interstitial solute clearance are more rapid during sleep and under circadian regulation, a process that at least in part is regulated via central noradrenergic regulation of the brain extracellular space volume (Xie et al., 2013; Ding et al., 2016; Hablitz et al., 2020). Quantitative measurements of cortical extracellular space volume using the tetramethylammonium iontophoresis method (Nicholson, 1992; Nicholson and Hrabětová, 2017) showed that the extracellular space increases from ~14% to 24% when awake mice transition into non-rapid eye movement (NREM) sleep or anesthesia (Xie et al., 2013). Whereas the extracellular space volume exhibited a sharp increase on loss of consciousness, the extracellular tortuosity remained unaltered (Xie et al., 2013; Ding et al., 2016). In slice preparations,

beta-andrenergic receptor activation reduced ECS volume and expanded astrocyting processes, as quantified using iontophoresis (Sherpa et al, 2016). Although these observations await independent confirmation, alternative methodologies, including electron microscopy, have supported the finding that cellular structures expand during wakefulness, restricting water diffusion (Rasmussen et al., 2021). Analysis of motor and sensory cortex in mice via electron microscopy documented that cortical synapses and perisynaptic astrocytic processes expand during wakefulness, and in particular, during sleep deprivation (de Vivo et al., 2017; Bellesi et al., 2015).

Diffusion weighted MRI studies have provided mixed results. One study in human brain was not able to detect changes in the mean diffusivity between wakefulness and sleep after sleep deprivation, thereby not corroborating extracellular space volume changes (Demiral et al., 2019). However, two other studies showed that 12 h of alert wakefulness during a learning paradigm led to a decline in cortical mean diffusivity. The decrease in water diffusivity became more pronounced during sleep deprivation combined with task practice. Ventricular volume decreased, whereas subcortical volumes of gray matter and white matter increased. All reported changes reverted after recovery sleep (Bernardi et al., 2016); moreover, human brain volume decreases steadily during wakefulness (Nakamura et al., 2015). Electroencephalography studies in rodents demonstrate that slow wave activity, indicated by low-frequency oscillations between synchronous activity and inactivity, is strongly associated with glymphatic function (Hablitz et al., 2019), suggesting that slow wave sleep is the phase of sleep during which glymphatic exchange is most rapid. The evolutionary basis for sequestration of glymphatic exchange and waste clearance into periods of sleep remains speculative. One possibility is that the reduced porosity ( $\sim$ 14%) in the waking brain is optimized for rapid and high-fidelity neuronal network activity, but suppresses solute efflux. The sleep-associated change in porosity, in turn, supports the clearance of metabolic wastes that accumulate through the waking day. The synchronous neuronal activity of slow wave sleep may drive fluid and solute movement physio-mechanically through coupled vasomotor changes. Such coupling has been observed between k complexes (isolated slow waves) during N2 NREM sleep and CSF movement through the ventricular compartment. Conversely, the intense but asynchronous network activity characteristic of the waking brain may prevent the organized movement of fluid and solutes through brain tissue. An interesting related case is the state of hibernation, which could be explored in future studies.

### *Clinical relevance of glymphatic dysfunction*

Neurodegenerative disease states such as Alzheimer's disease, Parkinson's disease, and Huntington's disease result in cognitive impairment and dementia, and are associated with distinct neuropathology in the form of accumulation of aggregation-prone misfolded waste proteins within the cytoplasm of neurons or deposited in the interstitial space of the neuropil. For example, extracellular amyloid beta plaques and intracellular tau aggregates are the central histological feature of Alzheimer's, whereas the abnormal accumulation and aggregation of $\alpha$-synuclein in the form of Lewy bodies are a central histological feature of Parkinson's. (The amyloid hypothesis for Alzheimer's disease is debated, however (Selkoe and Hardy, 2016).) The amyloid beta peptide is a normal product of amyloid precursor protein cleavage. Amyloid beta monomers can aggregate into different forms of oligomers, with sizes between 100 and 200 kD (Chen et al., 2017). Amyloid beta oligomers are soluble and can spread in the interstitial space of the CNS; however, when they convert into to a beta-sheet secondary structure, they fibrillize (Chen et al., 2017). Amyloid fibrils are insoluble and can assemble into amyloid beta plaques (Chen et al., 2017). However, there is a window of opportunity for removal of extracellular amyloid beta before it is incorporated into plaques. Stable isotope amino acid tracers in human subjects revealed that the amyloid beta turnover rate slowed with aging. Specifically, the half-life of all amyloid beta isoforms including A$\beta$42 was reported to decrease by 60%, from 3.8 h to 9.4 h over five decades of aging (Patterson et al., 2015), suggesting that the clearance mechanisms fail with aging and calling for therapeutic action. Furthermore, increased loss of soluble A$\beta$42 was noted in subjects already positive for amyloidosis, implying rapid and irreversible aggregation in the amyloid plaques (Patterson et al., 2015; Huang et al., 2012). In contrast to amyloid beta, tau is predominantly an intracellular soluble protein. However, tau has also been reported to be passively released by cells in disease and even across synapses in a prion-like manner (Annadurai et al., 2021; Goedert et al., 2017). Approximately 75% of tau in the human brain is of the full-length type whereas the rest is truncated (Sato et al., 2018). Notably, in CSF, tau is predominantly of the truncated type which is more aggregation prone (Sato et al., 2018; Kovacech and Novak, 2010). Kinetic analysis in humans revealed that the average half-life of tau is $\sim$ 23 days and the tau production rate is 26 pg/mL/day (Sato et al., 2018).

A key relationship between sleep disruption and Alzheimer's-related pathology has emerged recently as well. Clinical neuroimaging studies have shown that life-long sleep disruption and short sleep duration are associated with greater amyloid beta burden in the brain of elderly subjects (Spira et al., 2013), and even one night of sleep deprivation can elevate amyloid beta levels in the hippocampus of healthy subjects (Shokri-Kojori et al., 2018). The link between sleep and brain waste disposal has been further corroborated by studies from the Holtzman group showing that the concentration of amyloid beta in CSF is lowest during sleep and increases during wakefulness (Ooms et al., 2014). The same group also showed that disruption of slow wave activity increases CSF amyloid beta levels acutely, and poorer sleep quality over several days increases tau levels (Ju et al., 2017). Recent large scale studies similarly report that shorter habitual sleep duration is associated with increased tau and amyloid beta levels (Insel et al., 2021; Winer et al., 2021). The glymphatic system contributes to the clearance of soluble amyloid beta as well as tau (Iliff et al., 2012, 2014; Patel et al., 2019) and therefore constitutes a promising and alternative therapeutic target for curbing buildup of toxic waste protein and preventing cognitive impairment. This statement is strongly supported by several studies showing that the glymphatic system clears waste solutes in a manner dependent on the brain's state of arousal (Xie et al., 2013; Eide et al., 2021c; Eide and Ringstad, 2021), as well as cardiovascular and respiratory forces (Rennels et al., 1990; Annadurai et al., 2021; Goedert et al., 2017; Dreha-Kulaczewski et al., 2015, 2017), which are all therapeutically modifiable. More recent evidence in mouse models of Parkinson's demonstrate that pharmacological enhancement of slow wave sleep across several months can reduce pathological $\alpha$-synuclein accumulation and increase recruitment of AQP4 to perivascular sites, suggesting a possible relevant increase of glymphatic function also in Parkinson's (Morawska et al., 2021). Given this evidence, it is not surprising that the glymphatic system has gained tremendous interest in the neuroscience and clinical communities. As previously mentioned, the glymphatic system clears brain waste solutes — including amyloid beta and tau (Iliff et al., 2012, 2014) — in a manner dependent on the brain's state of arousal (i.e., sleep/wake cycle (Xie et al., 2013), anesthesia (Xie et al., 2013; Hablitz et al., 2019; Benveniste et al., 2017), and circadian clock (Hablitz et al., 2020)). Specifically, glymphatic solute transport was shown to increase during sleep and with certain anesthetics compared the wakefulness, and the increase is associated with elevated prevalence of slow delta activity (Xie et al., 2013; Ding et al., 2016).

Another common form of dementia in the elderly — vascular contribution to cognitive impairment and dementia (VCID) — involves pathology of the small vessels of the brain in the form of cerebral arteriosclerosis and is the most common cause of lacunar stroke and white matter loss. VCID is associated with enlarged perivascular spaces (PVSs) on T2-or T1-weighted MRI, and clinically, these are interpreted as CSF sitting "stagnant" along the vasculature (mostly arterioles) (Brown et al., 2018; Wardlaw et al., 2020). The enlarged PVS in VCID are now thought to indicate impaired glymphatic transport for a few reasons. First, glymphatic system transport is dependent on a healthy perivascular channel network to clear waste solutes. Accordingly, if the PVS is afflicted with disease (e.g., remodeled secondary to hypertension, inflammation, or diabetes) CSF flow and glymphatic function will be adversely impacted (Benveniste and Nedergaard, 2022). Second, in rodent VCID models perivascular CSF flow is sluggish (Koundal et al., 2020). Third, VCID rat models exhibit reduced parenchymal glymphatic transport (Koundal et al., 2020; Mortensen et al., 2019).

A more recent clinical area of interest involves the increased risk of perioperative delirium and cognitive dysfunction in elderly patients undergoing surgery, which is associated with significant morbidity and mortality. The potential role of CSF flow, solute waste, and glymphatic transport underlying its pathophysiology is now an active research area (Cunningham et al., 2019; Benveniste et al., 2019a; Hov et al., 2017; Idland et al., 2017). Indeed, the dependence of glymphatic function on choice of anesthetic regimen has been well documented, and this feature is related to the anesthetic drug's ability to induce slow wave delta activity (Hablitz et al., 2019) and also its ability to impair perivascular CSF transport by interfering with vasomotion and the physical dimensions of the PVS (e.g., vasodilation or vasoconstriction) (Ozturk et al., 2021). The various anesthetics used also have varying effects on vascular pulsatility, vascular compliance (cerebral vasoreactivity), and vasomotion, which are all key drivers of PVS CSF flow and glymphatic transport.

## Glymphatic biology: Questions raised

Glymphatic modeling and experiments have raised a number of questions that are subjects of ongoing debate in the literature. In our consensus view, some of the debates stem from knowledge gaps and could be resolved by specific future work, but other debates can largely be resolved with current knowledge. A few are discussed below.

### Diffusion and advection

Solutes are transported via diffusion anywhere concentrations are non-uniform and via advection anywhere fluid also flows. (We avoid the term "convection" because of ambiguity: It has sometimes been used as a synonym for advection, and sometimes to mean transport by the combined effects of advection and diffusion, which we denote "dispersion".) Thus, both processes almost certainly act throughout the glymphatic system, but their relative importance varies. It can be quantified by the Péclet number, $Pe = UL/D$, where $U$ is a characteristic flow speed, $L$ is a characteristic length scale, and $D$ is the diffusivity. When the value is very large ($Pe \gg 1$), advection dominates, as is typical for large molecules over long distances; when the value is very small ($Pe \ll 1$), diffusion dominates, as is typical for small molecules over short distances (Koundal et al., 2020; Ray et al., 2019; Valnes et al., 2020). There is consensus that solute transport in the larger perivascular spaces of the subarachnoid space occurs primarily via advection. Studies using DCE-MRI in combination with small-molecular-weight Gd-based tracers in CSF found advection dominating transport not only there, but also in the larger periarterial channels along arteries penetrating into the rodent brain (Iliff et al., 2013b; Koundal et al., 2020). Advection is also known to dominate transport along privileged pathways like white matter tracts (Iliff et al., 2012). Furthermore, regularized optimal mass transport (rOMT) analysis revealed high-speed transport suggestive of advection in the cerebellum, but not in the forebrain (Koundal et al., 2020), consistent with the facts that cytoarchitecture and blood vessel architecture differ from cerebellum to cortex, and that AQP4 expression is higher in cortex (Hubbard et al., 2015). The cerebellum is also very old from an evolutionary perspective (it occurs in lampreys), and its particular features might favor fast solute transport.

Whether advection is appreciable in the interstitial compartment remains an open question. Bulk flow in the interstitium would be necessary for conserving fluid mass if net CSF motion along periarterial spaces is directed into the brain. In the original description of the glymphatic system a small molecular weight solute (A594, with molecular weight 759 Da) was reported to distribute rapidly and almost ubiquitously across the mouse brain within $\sim$ 30 min (Iliff et al., 2012). This result, as well as other data obtained using *in vivo* two-photon microscopy and *ex vivo* optical imaging, led to the conclusion that transport of small-molecular-weight solutes in the glymphatic system, including the neuropil, was rapid and partly advective (Iliff et al., 2012; Nedergaard, 2013). However, this concept has since been challenged by several investigators (Jin et al., 2016; Smith et al., 2017; Abbott et al., 2018; Asgari et al., 2015, 2016; Holter et al., 2017). Recently it was suggested solutes move through brain parenchyma via diffusion down a concentration gradient maintained by perivascular advective flow (Thomas, 2019). Because glymphatic solute transport depends on what anesthetics are used in an experiment, comparison of results across laboratories has been difficult. We do know, however, that interstitial solute efflux depends on perivascular localization of AQP4 (Iliff et al., 2012; Mestre et al., 2018a) and is faster during sleep (Xie et al., 2013; Hablitz et al., 2019, 2020). The Cserr group showed that solute efflux occurs independently of molecular weight, which is a hallmark of advective transport (Cserr et al., 1981). Resolving the question of advective transport in the neuropil will require novel non-invasive approaches with high spatial and temporal resolution.

### The role of AQP4 in glymphatic function

AQP4 is an astroglial water channel that localizes primarily to the perivascular endfeet ensheathing the cerebral vasculature. Although implicated in early studies in the formation and resolution of cerebral edema following brain injury, the physiological role for this pattern of localization remained unclear. In the initial description of the glymphatic system in 2012, the authors reported that deletion of the AQP4 gene impaired perivascular CSF tracer influx and the clearance of interstitial solutes. In a subsequent study, Verkman et al. saw no effect from gene deletion on CSF tracer influx (Smith et al., 2017). Based on these findings, the role of AQP4 in perivascular fluid and solute exchange, and indeed the glymphatic model, were proposed to be refuted. However, a subsequent collaborative study aggregating data from five different research groups utilizing four separate null mouse lines found gene deletion affected both CSF solute influx and interstitial solute efflux (Mestre et al., 2018b). In addition, in this study, glymphatic function was impaired by deletion of the Snta1 gene, which results in the loss of perivascular AQP4 localization. An included meta-analysis demonstrates consistent results across comparable studies, excepting that of Verkman et al. Verkman et al. utilized different injection approaches than the other studies and an anesthetic regime that in previous work markedly suppressed glymphatic function (Hablitz et al., 2019). These results clearly establish the key role of the astroglial water channel AQP4 in perivascular glymphatic function and highlight the importance of using experimental methods, including injection protocols and anesthesia, that perturb physiological conditions minimally. The possible mechanisms by which AQP4 affects glymphatic flow are discussed in Interfaces to perivascular spaces, below.

*Directions of periarterial fluid flow and implications for cerebral amyloid angiopathy*

Observing that amyloid beta accumulates in the walls of penetrating and surface arteries in cases of cerebral amyloid angiopathy (CAA), Weller et al. proposed that the intramural spaces of the walls of the arteries serve as efflux pathways for interstitial solutes (Albargothy et al., 2018). Beginning with the initial description of the glymphatic system in 2012, and in subsequent studies from multiple groups in both rodents and humans, the observed influx of CSF solutes into brain tissue along perivascular spaces surrounding arteries, and the clearance of interstitial solutes like amyloid beta along perivenous and white matter tracts towards sinus-associated cisternal CSF compartments, appeared to contradict this periarterial efflux route. More recently, Carare et al. have reported that intra-parenchymally injected tracers, including amyloid beta, localize to the basement membranes of arteries and veins as early as 30 min after injection (Albargothy et al., 2018; Carare et al., 2008). The divergent findings of amyloid beta clearance along veins versus arteries have led to controversy in the field of brain waste clearance (Abbott et al., 2018; Agarwal and Carare, 2020; Benveniste et al., 2019b; Hladky and Barrand, 2018; Mestre et al., 2020b). The periarterial clearance concept — referred to as the intramural periarterial drainage (IPAD) model — states that glymphatic influx of CSF (including soluble amyloid beta) occurs along the basement membranes on the outside of the artery walls, and the clearance of amyloid beta from the neuropil happens along the basement membrane of capillaries, continuing upstream into the basement membranes of smooth muscle cells within the walls of arterioles and arteries (Albargothy et al., 2018; Aldea et al., 2019). There are several pieces of information that are important to contextualize for understanding these two opposing viewpoints.

First, there is general consensus that small molecular weight CSF solutes and waste including tau drain via the glymphatic system from the CNS via meningeal and extracranial lymphatics (Engelhardt et al., 2016; Aspelund et al., 2015; Louveau et al., 2015; Ahn et al., 2019; Patel et al., 2019; Eide et al., 2018). Second, although the exact anatomical constructs connecting the glymphatic and lymphatic systems are still actively investigated, recent data from human brain acquired using DCE-MRI show that Gd-based tracers from CSF and brain parenchyma egress the CNS partly via a transitional hub, the parasagittal dura, which runs along the superior sagittal sinus (Ringstad and Eide, 2020), implying that waste clearance is indeed perivenous. These clinical studies are supported by data in rodents revealing the existence of an extensive network of meningeal lymphatic vessels with valves along the sigmoid and petrosquamosal venous sinuses and in the dura covering the skull base, which drain to the cervical lymph nodes (Ahn et al., 2019). Furthermore, the dorsal and ventral meningeal lymphatic vessels may serve as connective hot spots for glymphatic egress of macromolecules from the brain parenchyma or CSF (Ahn et al., 2019; Rustenhoven et al., 2021), implying that there are direct connections between the two systems. That said, the precise distribution of CSF drainage by lymph vessels is not yet known. Ahn et al. (Ahn et al. (2019) argued that basal meningeal lymphatic vessels carry more CSF than dorsal ones, and Ma et al. (Ma et al. (2017) found no tracer uptake by dorsal meningeal lymphatic vessels. Further studies will clarify the relative importance of the various vessels in clearing CSF.

Third, the IPAD model is grounded in the neuropathological signature of CAA (Albargothy et al., 2018; Carare et al., 2008; Agarwal and Carare, 2020), the rapid association of injected amyloid beta with arterial basement membranes, and an anatomical division between glymphatic influx along arterial perivascular spaces and the intramural basement membrane. CAA presents as two subtypes: CAA type 1, where amyloid beta accumulates along cerebral microvessels and capillaries, and CAA type 2, where amyloid beta accumulation occurs within the walls of small arteries and arterioles, primarily in the leptomeninges and cortex (Thal et al., 2002). At least initially, it has seemed difficult to reconcile the deposition pattern of amyloid beta in CAA type 2 with the glymphatic model including perivenous drainage. However, the clearance of a solute along a pathway is likely to preclude accumulation along that pathway. It is possible that the deposition of amyloid beta in arterial walls reflects retention because of matrix interactions or perhaps the stagnation of periarterial influx, rather than the physiological route for amyloid beta clearance. Indeed, CAA is clinically associated with greater perivascular space dilation. A similar critique applies to the studies reporting rapid association of injected amyloid beta with arterial segments. It is possible that this rapid association reflects binding and retention of amyloid beta with arterial basement membranes or is an artifact of the intraparenchymal injection technique. Because these studies were not carried out with time-resolved imaging, it is difficult to compare them with the dynamic imaging studies that have demonstrated periarterial CSF tracer influx. In addition, tracer can move great distances and enter different tissue during death (Mestre et al., 2020a) and perfusion (Mestre et al., 2018a), so postmortem imaging is unavoidably prone to significant artifacts.

Substantial intramural flows along arterioles would also seem to be prevented by fluid dynamics. Intramural spaces in arteriole basement membranes have lateral sizes on the order of 100 nm (Keith Sharp et al., 2019), whereas perivascular spaces have lateral sizes of a few microns around murine penetrating vessels (Iliff et al., 2012), 40 $\mu$m around murine pial vessels (Mestre et al., 2018a), and 300 $\mu$m around human pial vessels (Bedussi et al., 2018). For flow in any of these spaces, all else being equal, the volume flow rate scales as the lateral size to the fourth power, according to the Hagen-Poiseuille equation. Thus, estimating the size of the space in the arteriole basement membrane to be smaller than the perivascular space by a factor of $10^2$, we expect that, in each minute, the volume of fluid carried along the basement membrane is less than that carried along the perivascular space by a factor of $10^8$. Fluid flows hypothesized to occur in basement membranes, if they exist, are therefore likely to cause so much less transport than observed perivascular flows as to be negligible and probably unmeasurable.

Lastly, although the IPAD model presupposes a functional separation between arterial PVS influx routes and intramural efflux routes, its anatomical basis remains unclear. The initial study characterizing glymphatic function in the rodent brain clearly demonstrated that fixable CSF tracers entering along periarterial influx routes had relatively unrestricted access to the basement membranes between the vascular smooth muscle cells and the underlying endothelial cell layer. However, the relationship between glymphatic function and dysfunction and the occurrence of CAA remains poorly understood. One possible explanation could be that amyloid beta oligomers taken up by phagocytotic vascular smooth muscle cells act as the seeds that initiate vascular amyloidosis (Soltoff-Schiller et al., 1976). Another explanation could be that the reduction in glymphatic flow in aging (Kress et al., 2014), combined with a multitude of age-related changes, including stiffening of the arterial wall, enlargement of the perivascular spaces, reactive gliosis, and changes in intracranial pressure (Wen and Wong, 2019), may lead to stagnation of periarterial fluid, increasing the likelihood of amyloid beta aggregation. Clearly, further experiments are required to understand the underlying mechanisms for waste deposition patterns in CAA, in particular CAA type 2.

### *In vivo* approaches that inform glymphatic modeling

Seeing that many of the outstanding questions for glymphatic modeling can be resolved only with the help of additional experimental measurements, having noted that measurements can depend sensitively on experimental technicalities like anesthesia type and injection protocols, and having pointed out that postmortem measurements may not reflect the biology of living animals, here we present practices that can help future experimental studies maximize their benefit for modeling.

The glymphatic system relies on three steps to function: influx of CSF via perivascular spaces, mixing of CSF with ISF, and clearance of the fluid that has travelled through brain tissue. The first two steps are the focus of most glymphatic assays and have been shown to vary greatly in disease models. The initial discovery of the glymphatic system was made using dynamic two-photon imaging *in vivo* (Iliff et al., 2012), which has been further developed to track the movement of individual particles (Mestre et al., 2018a). Two-photon microscopy offers excellent resolution (0.5 to 1 $\mu$m in-plane, 1.5 $\mu$m out-of-plane) but with limited tissue penetration (to 200 $\mu$m or a bit more, depending on contrast), and the frequent need for a cranial window (Figure 2).

Imaging of the entire dorsal cortex can be performed using epifluorescence microscopy through an intact skull. This approach is valuable for tracking perivascular CSF tracer influx and for studies in awake mice. The main limitation of this type of macroscopic imaging is its lack of depth information, particularly its inability to distinguish tracers in the subarachnoid space from those in cortical tissue (Plog et al., 2018).

Light sheet microscopy has allowed 3D imaging of the entire rodent brain (Bèchet et al., 2020) and parts of a pig brain (Bèchet et al., 2021), with the potential for slightly larger brains. Such imaging gives access to parameters including average influx depth and number of influx sites per cortical area, while causing little photobleaching or phototoxicity. Observing variations in time can be difficult, however, because light sheet imaging cannot be done *in vivo*.

Tracer influx can also be imaged in postmortem brain slices, using equipment that is readily available in many laboratories, with high resolution. However, time-lapse imaging is not possible, so death effects again complicate data interpretation, and sample collection is labor-intensive (Figure 2). Although most optical imaging is centered on studying influx of CSF tracers, assays for efflux are being developed (Iliff et al., 2013a; Lee et al., 2015; Evans et al., 2020; Stanton et al., 2021).

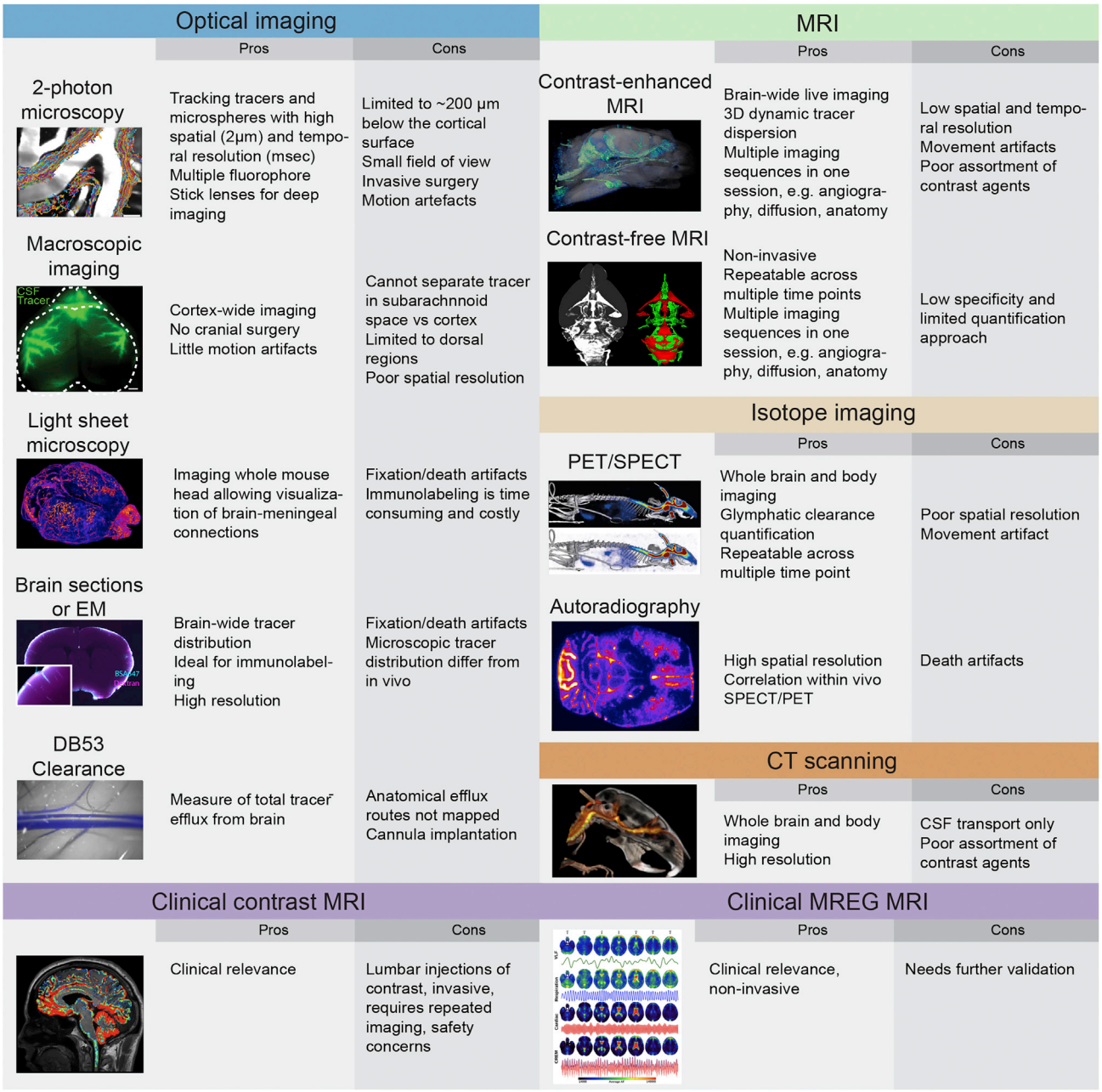


**Figure 2. Overview of experimental techniques that can inform glymphatic modeling**

[1]In spite of the mathematician Gelfand's claim that "there is only one thing which is more unreasonable than the unreasonable effectiveness of mathematics in physics, and this is the unreasonable ineffectiveness of mathematics in biology", the powerful mathematical methods developed with the understanding of inorganic matter are often surprisingly useful (Wigner, 1990).

MRI techniques can provide global, time-lapse imaging which enables investigations of both influx and efflux rates. MRI can detect glymphatic function by measuring signal from paramagnetic ($Gd^{3+}$) tracers or from brain water itself (phase contrast MRI, blood-oxygen-level-dependent (BOLD) MRI). Experiments show $Gd^{3+}$ tracers are distributed brain-wide in less than 24 h, with timing varying among diseases (Ringstad et al., 2017, 2018; Eide et al., 2021b) and with sleep (Eide and Ringstad, 2021). Novel high-speed techniques can measure flow (Dreha-Kulaczewski et al., 2017) and tissue deformation (Sloots et al., 2020) on short timescales. Recent studies have used BOLD techniques to measure motions of free CSF (Posse et al., 2013; Kiviniemi et al., 2016; Fultz et al., 2019; Hennig et al., 2020). However, MRI imaging in animals

that are not anesthetized can be difficult to interpret, because the loud noises made by MRI machines may induce a stress response in animals (Cai et al., 2020). Computed tomography (CT) and positron emission tomography/single-photon emission computed tomography (PET/SPECT) scans may also prove to be viable ways of measuring CSF tracer influx and clearance *in vivo* (2).

Recently-developed super-resolution microscopy techniques enable optical imaging with resolution well beyond the diffraction limit through the use of fluorescent tracers. Single-molecule localization microscopy (SMLM) works by inducing fluorescence in a small, isolated tracer, such as a carbon nanotube, and has been used in acute brain slices to reveal significant local variations in the spaces between cells, with implications for the porosity and tortuosity of brain tissue (Godin et al., 2017). When tracer molecules cannot be isolated, resolution can still be increased by reducing the effective size of the laser spot that excited fluorescence, as in stimulated emission depletion (STED) microscopy, which has been used to visualize neurons and glia (Arizono et al., 2020; Nägerl et al., 2008) as well as the structure of the extracellular space surrounding them (Tønnesen et al., 2018). Technical challenges have so far prevented *in vivo* use of these super-resolution techniques but may soon be overcome.

Beyond the question of imaging techniques, accurate study of the glymphatic system requires carefully avoiding creation or alteration of pressure gradients in the brain, because even small gradients can drive substantial flow. For example, craniectomy without penetration of the dura mater impairs glymphatic circulation (Borha et al., 2020; Plog et al., 2020). In one study, preparation of a cranial burr hole and insertion of a glass pipette through the dura mater and into the brain parenchyma suppressed CSF tracer influx by 40% (Mestre et al., 2018b). Many imaging methods involve invasive injection of tracer into the cisterna magna. Leaving the needle in place during experiments reduces acute trauma. Still, tracer injection can increase the intracranial pressure (ICP), and many researchers have noted the potential for that increase to drive artifactual flows (Smith et al., 2017; Keith Sharp et al., 2019; Smith and Verkman, 2018; Croci et al., 2019; van Veluw et al., 2020; Vinje et al., 2020; Kedarasetti et al., 2020b; Faghih and Keith Sharp, 2021). One recent study found that after injecting 10 $\mu$L of fluid at a rate of 2 $\mu$L/min into the cisterna magnas of mice, ICP increased by 2 mmHg (Raghunandan et al., 2021). Theoretical estimates predict that if the pressure were 2 mmHg higher in one region of the murine skull than in another, robust fluid flow would ensue. On the other hand, a spatially uniform ICP change would cause no flow at all. Moreover, ICP variations greater than 2 mmHg occur when mice change their body position or sneeze (Lee et al., 2015). In further experiments in the same study, 20 $\mu$L was injected at 2 $\mu$L/min while fluid was simultaneously withdrawn at the same rate through a second cannula. In those experiments, ICP did not change over time, but flow in pial PVSs were statistically indistinguishable from the earlier experiments, suggesting that injecting 10 $\mu$L into the murine cisterna magna at 2 $\mu$L/min perturbs flows minimally (Raghunandan et al., 2021). More broadly, since flow is driven not by ICP but by its spatial variation, and because *in vivo* measures of that spatial variation have been achieved only twice (Eide et al., 2012; Young et al., 2021), using future models to estimate pressure variation could substantially advance the field.

That said, pressure changes are not the only perturbations that can be caused by invasive imaging techniques, and we urge the use of noninvasive techniques whenever possible.

## MECHANISMS

Because the glymphatic system comprises a brain-wide, coordinated network for fluid and solute transport, modeling it meaningfully requires considering both global and local effects and accounting for a wide variety of mechanisms. Although an exhaustive discussion of all mechanisms would be impossible until much ongoing and future work is completed, we highlight key mechanisms. The discussion in this section is about the mechanisms themselves, their implications, and what we know about them from prior work; actually modeling them is the topic of the next section. The mechanisms comprise the entire glymphatic pathway: flow in PVSs, transport in brain parenchyma, links between PVSs and parenchyma, and brain efflux routes. The section concludes with a discussion of mechanistic links to neuronal activity.

### Perivascular flow

In the glymphatic model, CSF enters the brain along periarterial spaces, so our discussion of drivers and modulators begins there. Given decades of *in vivo* evidence of flow in perivascular spaces, it is natural to wonder what fluid dynamical mechanisms propel CSF and set its net flow direction. Pumping mechanisms are known most clearly for the pathological cases of stroke and cardiac arrest, in which *in vivo*

flow measurements can be matched reasonably closely, at both local and global scales, by assuming that flow is driven by the contraction of arteries with the passing of a wave of spreading depolarization (Mestre et al., 2020a; Du et al., 2022).

Physiological pumping mechanisms are less certain, and many have been proposed. Although respiration modulates lymphatic flow and is expected to influence CSF flow in perivenous spaces (Santisakultarm et al., 2012) and ventricles (Fultz et al., 2019; Vinje et al., 2019), flow in periarterial spaces evidently pulses in synchrony with the heart (Mestre et al., 2018a; Bedussi et al., 2018); respiration seems to play a role only incidentally, when it occurs in step with the heartbeat (Mestre et al., 2018a). Similarly, another recent study found that strong respiratory pulsations in the human brain modulate cardiac pulsations in central CSF spaces (Raitamaa et al., 2021). Given the synchrony between periarterial flow and the heart, it has long been hypothesized that the waves of constriction and dilation that travel down artery walls with each heartbeat (now detectable with MRI (Rajna et al., 2021; Tuovinen et al., 2020)) might drive not only CSF oscillation but also a net motion of CSF in periarterial spaces, parallel to the blood (Hadaczek et al., 2006; Wang and Olbricht, 2011), in a mechanism dubbed "perivascular pumping". Experiments have demonstrated that in physiological conditions, artery wall velocities closely match CSF velocities in pial perivascular spaces, and that altering artery wall motion (by raising the blood pressure to cause arterial stiffening) significantly reduces CSF flow (Mestre et al., 2018a), suggesting that artery wall motion at the cardiac frequency plays an important role. On the other hand, one team has also pointed out that net CSF flow antiparallel to blood could occur in certain cases of wave reflection (Coloma et al., 2016, 2019). Net flow might also be driven in part or entirely by the global change in cranial blood volume with each heartbeat, which would likewise produce lock-step synchrony with the heart, as observed *in vivo*. To the extent that cardiac pulsations cause CSF flow, arrhythmia might lead to pathological glymphatic function; future studies should address this possibility.

Another alternative is that cardiac pulsation and blood volume change drive oscillations but not the observed net flow, which is caused by other mechanisms. Even small pressure gradients, on the order of 1.5 mmHg/m, would be sufficient (Kedarasetti et al., 2020b; Daversin-Catty et al., 2020). Actual pressure gradients are not well-known. Eide et al. (2012) measured ICP simultaneously at two locations in the human skull, finding differences of a few mmHg. Young et al. (2021) measured ICP simultaneously in the cranial and spinal subarachnoid spaces of alligators, finding differences of similar magnitude. To our knowledge, no other studies have measured ICP at more than one location simultaneously, so making accurate estimates of pressure gradients is difficult. Linninger et al. (2009) used temporal pressure variations and model parameters to estimate that pressure differences among brain CSF compartments might be as large as 1 mmHg, agreeing with the experimental measurements (Eide et al., 2012; Young et al., 2021). If present in a $\sim$10 mm mouse brain, such pressure differences would imply pressure gradients significantly larger than the 1.5 mmHg/m required to drive observed flows. Thus, it is useful to consider mechanisms that might cause steady pressure gradients.

One such mechanism is functional hyperemia, the process by which additional blood is routed to active regions of cortex, depending on brain state (Fultz et al., 2019; Kedarasetti et al., 2020a). The corresponding vasodilation would displace CSF in perivascular spaces unless the outer boundaries expand by the same amount, which is unlikely. However, like cardiac pulsation, functional hyperemia could drive oscillations without net flow, albeit on longer timescales. Early work proposed that fluid secretion across the blood-brain-barrier could drive flow (Cserr et al., 1981; Bradbury and Cole, 1980) in the parenchyma, and secretion has recently been measured via MRI, suggesting CSF is produced not only near choroid plexus but also in the subarachnoid space (Petitclerc et al., 2021). By extension, secretion might drive flow in perivascular spaces as well, but it has not been measured directly and can be estimated only roughly (Hladky and Barrand, 2014, 2018), so we will not discuss it further. However, a recent study based on direct measurements of CSF production in mice found that production and glymphatic fluid transport are regulated differently and can change independently (Liu et al., 2020). In any case, the relative importance of flow drivers almost certainly varies by location and depends on brain state.

Another mechanism is CSF production by the choroid plexus, which presumably involves an osmotic pressure sufficient to drive some flow. Osmotic (Starling) forces are considered in (Buishas et al., 2014; Linninger et al., 2017), which make ambitious attempts at global modeling of the water and solute transport through the brain. Osmotic forces require membranes over which they can act, and the membranes considered are in choroid plexus, blood brain barrier, extracellular spaces, pia mater, and the lining around the ventricles.

The characteristics of perivascular spaces affect flows there and can inform models of potential pumping mechanisms. Because veins lack smooth muscle cells and are compliant, they seem less likely to pump perivenous fluid, although blood volume changes might still play a role; additional experimental study is needed. Crucially, the porosity of perivascular spaces likely varies from proximal to distal parts of the glymphatic system; pial periarterial spaces are known to be open (not porous) (Min Rivas et al., 2020), but elsewhere, the porosity is unknown. Shapes also matter. Pial periarterial spaces typically have elliptical cross-sections (Mestre et al., 2018a; Bedussi et al., 2018; Schain et al., 2017), whereas penetrating periarterial spaces typically have nearly circular cross-sections with their arterioles placed eccentrically to one side. Both shapes have lower hydraulic resistance (pressure drop per volume flow rate) than circular concentric annuli of the same size (Tithof et al., 2019). With perivascular pumping, elliptical cross-sections would cause azimuthal flow — pulsatile fluid motions along orbits around the axis of the artery (Thomas, 2019; Carr et al., 2021; Coenen et al., 2021). Also, pial periarterial spaces can communicate directly with pial perivenous spaces (Bedussi et al., 2017), are connected via more anastomoses, and are larger than penetrating periarterial spaces. Periarterial spaces are commonly thought to attenuate and end before reaching the capillaries, but pericapillary spaces have been speculated to exist (Hannocks et al., 2018; Ferris, 2021) and would presumably have characteristics different from either pial or penetrating periarterial spaces.

## Transport in brain parenchyma

If tissues throughout the brain rely on fluid transport to eliminate waste and deliver nutrients, then much of that transport must occur in brain parenchyma, and particularly, in the extracellular space (ECS). Transport there has often been measured using radiotracers, and more recently using two "point-source paradigms". The latest technical approach utilizes single particle tracking of carbon nanotubes. A review of transport in the ECS appeared in 2008 (Syková and Nicholson, 2008), and more recent ones are now available (Nicholson and Hrabětová, 2017; Soria et al., 2020; Sun and Sun, 2021).

These measures typically presume that diffusion dominates transport in the ECS, consistent with the fact that advection is relatively weak for transport of small molecules over short distances (see Section Rapid review). Diffusion analysis provides three pieces of information. The first is an effective diffusivity in the brain for a given molecule, such as a metabolic waste product, drug, or probe molecule (see (Syková and Nicholson, 2008; Fenstermacher and Kaye, 1988) for selected values). The second is the porosity (volume fraction) of the ECS, defined as $\alpha = V_{ECS}/V_{total}$, the ratio of the ECS volume $V_{ECS}$ to the total tissue volume $V_{total}$. The third is the tortuosity, which is a measure of the hindrance that a molecule experiences because of the structure of the brain. Tortuosity is defined as $\lambda = \sqrt{D/D^*}$, where $D$ is the free diffusivity of a molecule and $D^*$ is the effective diffusivity in brain tissue. Both porosity and tortuosity are characteristics of the ECS structure.

The radiotracer method was developed by Rall, Fenstermacher and Patlak in the 1970s (Fenstermacher and Kaye, 1988). In it, the ventricles of an anesthetized animal are perfused with a radiotracer that spreads into adjacent brain regions. After a chosen time, the animal is euthanized and the brain fixed. Then, small samples of tissue are taken along a path normal to the surface of the brain, and the radiotracer content is counted in each sample and analyzed using a solution to the diffusion equation. Studies with sucrose and inulin showed that $\alpha$ was 18% to 20% in the cerebral cortex in several species (Levin et al., 1970) and $\lambda$ was $\sim$1.5 in the dog caudate nucleus (Fenstermacher and Patlak, 1976). The major disadvantages of this method are that there is only one time point per animal and tissue samples are 0.5 mm to 1 mm thick, so spatial resolution is low.

In the context of the glymphatic system, Rosenberg et al. (Rosenberg et al. (1980) used the radiotracer paradigm to look for bulk flow in the ECS in cat caudate nucleus. They concluded that there was flow in white matter bundles with a velocity of 10.5 $\mu$m/min but zero flow velocity in gray matter. The gray matter measurements were criticized by Cserr et al. (Cserr et al. (1981) because they did not account for the vectorial nature of flow. Ultimately, the radiotracer method is unlikely to be sensitive enough to reveal reliable flow data.

The "point-source paradigm" was first realized in the real time iontophoresis (RTI) method introduced by Nicholson and Phillips (Nicholson and Phillips, 1981). A small extracellular probe ion, typically tetramethylammonium, was released from a micropipette by iontophoresis and the concentration measured $\sim$100 $\mu$m away using an ion-selective microelectrode. The parameters $\alpha$ and $\lambda$ were extracted by fitting

a solution of the diffusion equation to the concentration verses time curves. Measurement time was of the order of a minute, enabling real-time changes in brain environment to be monitored. The RTI technique confirmed that $\alpha$ was about 20% and $1.5 \leq \lambda \leq 1.6$ in several brain regions in rats, mice, and other species (Syková and Nicholson, 2008). These results were obtained in anesthetized animals or brain slices. When measurements were made in awake mice $\alpha$ was found to be only 14% (Xie et al., 2013). In contrast, in ischemia or anoxia, $\alpha$ fell to about 5% (Syková and Nicholson, 2008), which is typically the value seen in classical electron microscopy, where the ECS is known to be largely obliterated. Limitations of the RTI method include the fact that it can only be used with a few small charged molecules and requires an invasive procedure that may alter transport.

The point-source paradigm was extended to macromolecules with the introduction of the integrative optical imaging (IOI) method (Nicholson and Tao, 1993). A micropipette was again used as a source and a small volume of fluorescently labeled molecules pressure injected into brain tissue. The resulting cloud was imaged, and the intensity distribution fitted to a solution to the diffusion equation enabling $\lambda$ to be extracted. An important finding was that $\lambda$ increased with molecular size. This increase was attributed to interaction with the "walls" of the ECS, an interpretation bolstered by applying restricted diffusion theory, which also indicated an ECS average width of about 40 nm (Nicholson and Hrabětová, 2017; Thorne and Nicholson, 2006).

Ray et al. (Ray et al. (2019) showed that variation in a set of *in vivo* RTI measurements could be matched more accurately with a model that included, in addition to diffusion, advective transport with superficial flow speeds as high as 50 $\mu$m/min. However, similar experimental variability occurs in RTI measurements in brain slices, where no flow is expected. If such flows do occur, we would expect advection to cause solute transport at rates similar to diffusion, if a bit less, as evidenced by the Péclet number: taking $U = 250\ \mu$m/min ( $= U_s/\alpha$, with superficial speed $U_s = 50\ \mu$m/min and porosity $\alpha = 0.2$), $L = 250\ \mu$m (a typical separation distance between penetrating vessels in the cortex) and $D = 0.18\ \mu m^2$/ms for A$\beta$42 (Waters, 2011) gives Pe = 5. Thus, both diffusion and advection would contribute significantly to A$\beta$42 transport in the ECS. Of the point-source measurement methods, IOI would be more likely to detect advection effects because it uses larger molecules (hence, smaller $D$ and larger Pe). RTI, which uses small molecules, would be affected much less. MRI, perhaps in combination with rOMT, may be a more promising method for quantifying flow in the ECS (see Section Quantifying and defining glymphatic transport with optimal mass transport).

The idea that osmotic pressure differences could be a basic mechanism for transport in the brain parenchyma has been explored recently by Halnes et al. (Halnes et al. (2019). Previously, some of the same authors developed a scheme for the quantifying concentrations of $Na^+$, $K^+$ and $Cl^-$ in the ECS (Halnes et al., 2013). The more recent paper considered how ion dynamics could drive flow by osmosis across astrocyte membranes, which have high permeability thanks to AQP4 channels. With concentration differences around 60 mM, osmotic pressure differences were predicted to reach 1000 mmHg, which would dominate all other pressure differences in the ECS. Thus, osmotic flows might play a key role in the glymphatic system, and further study is warranted.

Recent studies show that ECS volume can change dynamically during physiological and pathological events on multiple time scales: over a day (sleep-wake cycle), over minutes (spreading depolarization), and in seconds (epilepsy). The volume fraction ($\alpha$) is about 20% in anesthetized animals and brain slices so it was a surprise when Xie et al. (Xie et al. (2013), using the RTI-TMA method in mouse cortex, found that $\alpha$ changed from 23% to 14%, as the sleeping animal awoke. This state transition is mediated by noradrenergic innervation (Constantinople and Bruno, 2011), and Sherpa et al. (Sherpa et al, 2016) confirmed that activation of adrenergic receptors in brain slices reduced $\alpha$ from 22% to 18%. Spreading depolarization (SD; also known as spreading depression) is an abnormal transient depolarization of a population of brain cell that propagates at about 3 mm•min$^{-1}$ in the cortex and elsewhere (Somjen, 2001; Lauritzen and Strong, 2017). SD-like events can occur in migraine headaches, ischemia, trauma, and seizures (Somjen, 2001; Lauritzen and Strong, 2017; Hartings et al., 2017). The ECS shrinks dramatically during SD (Van Harreveld and Khattab, 1967; Phillips and Nicholson, 1979) and Hrabe and Hrabetova (Hrabe and Hrabetova, 2019) introduced time-resolved IOI and showed that diffusion of a small extracellular marker (3000 Da) briefly ceased at the peak of SD. Epileptic seizures represent abnormal synchronous excitatory activity in neurons. Colbourn et al. (Colbourn et al. (2021) infiltrated the ECS with tetramethylammonium and used ion-selective

microelectrodes to reveal a new phenomenon they called rapid volume pulsation (RVP). This transient reduction of $\alpha$ coincided with the local field potential spikes of epileptic activity. The studies of sleep, SD, and seizure demonstrate that the volume of the ECS compartment can change in response to brain activity over a range of timescales.

Super-resolution fluorescence microscopy enables live imaging of fluorescent probes beyond the classic diffraction limit of light microscopy. Two implementations are especially relevant to the ECS. The first is single molecule light microscopy exemplified by the use of single-walled carbon nanotubes (Godin et al., 2017; Paviolo et al., 2020) that are intensely luminescent, photostable, and work in the near-infrared. The nanotubes are highly elongated and diffuse slowly, enabling single-molecule tracking. Application in acute brain slices reveals local ECS to be very heterogeneous, with many inter-cellular gaps greater than 100 nm. In addition, nanotube imaging can distinguish the geometric and viscous components of diffusion and look at structural changes (Godin et al., 2017; Soria et al., 2020; Paviolo et al., 2020). The second super-resolution implementation is point-spread function engineering that optically shrinks the fluorescent spot, achieving a spatial resolution of tens of nanometers, exemplified by STED microscopy (Arizono et al., 2020; Nägerl et al., 2008). To apply this to the ECS, Nägerl et al. combined 3D-STED microscopy with a diffusible, membrane-impermeable, fluorescent dye in the ISF, and called the method super-resolution shadow imaging (SUSHI) (Tønnesen et al., 2018). This technique enabled visualization of ECS structure in organotypic slices derived from mouse hippocampus (Arizono et al., 2020; Tønnesen et al., 2018; Paviolo et al., 2020). The width of the local ECS measured by SUSHI was highly heterogeneous, ranging from below the 50 nm resolution limit of SUSHI to above 1 $\mu$m. Most gaps exceed 100 nm, in agreement with electron microscopy of cryofixed tissue (Korogod et al., 2015) and nanotube imaging. Local ECS volume fraction averaged around 20%. After technical limitations are overcome, these two super-resolution techniques should work in the intact brain *in vivo*; already, however, they reveal heterogeneity of the ECS on a nanoscopic scale that may impact glymphatic models.

## Interfaces to perivascular spaces

Meaningfully modeling solute transport in the parenchyma requires accounting for phenomena at the interfaces between parenchyma and perivascular spaces. Likewise, meaningfully modeling flow (and transport) in PVSs requires accounting for phenomena at those same interfaces, as well as the proximal interfaces between PVSs and other fluid compartments. A few mechanisms are known to have important implications.

First, consider interfaces between PVSs and other fluid compartments. In experiments, tracer is often injected into the cisterna magna, but not all CSF there, or in subarachnoid spaces, is drawn into PVSs. Rather, two studies found that for small tracers, approximately 20% enters the brain (Xie et al., 2013; Lee et al., 2018). The percentage is probably smaller for larger tracers because influx of a CSF tracer is an inverse function of its molecular weight. A more recent study used a heavy isotope of water, $H_2^{17}O$, with molecular weight just 19 Da, orders of magnitude less than common contrast agents or fluorescent dyes, and found much more than 20% influx (Alshuhri et al., 2021). Small molecular weight, however, may not be the sole cause of the observed difference because many membranes pass water but block other molecules, e.g., via AQP4. Moreover, subarachnoid CSF is not the only source of ISF: Vascular fluid crosses the blood-brain-barrier to form additional ISF (Petitclerc et al., 2021). This idea is debated, and albeit no definitive proof has been presented, it is estimated that the contribution of vascular fluid to ISF is in the range of 20 to 100% (Rasmussen et al., 2021). Based on these lines of evidence, it can be concluded that ISF is not static but rather constantly being exchanged with surrounding fluid compartments, both CSF and blood.

Second, consider interfaces between PVSs and parenchyma. AQP4 water channels are known to cover much of the endfoot surfaces that separate PVS from parenchyma (Nagelhus et al., 1998), and eliminating that localization or knocking out AQP4 altogether is known to reduce glymphatic flow (Iliff et al., 2012; Mestre et al., 2018b), but the neurological mechanism by which AQP4 regulates glymphatic flow is a topic of ongoing study. One hypothesis is that water passes from periarterial spaces, into astrocyte bodies via AQP4 channels, through the cells, and out again to perivenous spaces and/or nerve sheaths. A second (and not exclusive) hypothesis is that water and solutes pass from periarterial spaces into parenchyma through the gaps between astrocyte endfeet, with flow in the gaps being somehow controlled by AQP4. (Because AQP4 is specifically a water channel, solute molecules cannot pass through it directly.) Both of

these hypotheses depend sensitively on the size, arrangement, composition, and biological activity of the endfeet, which are difficult to image *in vivo*. Furthermore, AQP4 is highly polarized, with a high localization at the endfeet, where a high percentage of the surface is covered by AQP4 (Nagelhus et al., 1998; Nielsen et al., 1997). However, the endfeet comprise only a fraction of the astrocyte membrane area. In fact, more than 90% of the total surface area of the astrocyte is estimated to be in the processes. As such it is hard to assess the relative importance of endfoot resistance, compared to that of the intra-cellular pathway. Although AQP4 is a highly selective water channel, the endfoot gaps are $\sim$20 nm wide and allow for the passage of a range of small molecules as well. For example, amyloid beta typically has diameter of a few nm and could pass, although its oligomerized length may be $\sim$100 nm. As such, the perivascular-parenchyma interface can be understood as a semi-permeable membrane involving both intra- and extracellular compartments, where both hydrostatic and osmotic pressure gradients may play crucial roles (Asgari et al., 2015), dependent on the astrocyte geometry and AQP4 localization. Furthermore, it has recently been shown that the size of astrocyte endfeet varies along the vasculature (Wang et al., 2021), correlating with vessel diameter. In simulations, that variation allowed near-constant flux through the endfoot gaps across the vascular generations.

Alternatively, if pericapillary spaces exist (Hannocks et al., 2018; Ferris, 2021), they might provide a continuous fluid pathway from periarterial spaces to perivenous spaces without entering the ECS. Further anatomical studies could clarify the situation.

### Efflux routes

CSF influx routes have been extensively studied by optical or MR imaging approaches, yet only a few studies have dissected the path by which ISF exits the CNS (Rasmussen et al., 2021; Steven, 2021). Taking the law of conservation of mass into consideration, however, we can deduce that a large volume of fluid must be leaving the CNS: efflux must match influx. Multiple paths for fluid efflux exist, including the perivenous spaces, spaces along cranial and spinal nerves, subarachnoid granulations, and more (Rasmussen et al., 2021; Steven, 2021). The exported fluid is ultimately collected by lymphatic vessels and returned to the general circulation close to the subclavian veins. Very few studies have attempted to quantify the relative importance of the different efflux paths. In fact, it is likely that the relative volume of fluid leaving CNS by any of the efflux routes constantly changes in response to body position (Lee et al., 2015), state of brain activity, and changes in ICP. Efflux is also likely to vary in the long term, depending on age, cardiovascular health, and disease. Classical studies concluded, based on injection of radiolabeled compounds, that only a minor fraction of ISF mixes with CSF before leaving CNS (Cserr et al., 1981), but these studies await confirmation using less invasive approaches. The importance of efflux via subarachnoid granulations is also debated, as the granulations do not exist in early childhood and might be absent in most experimental animal models, including rodents.

### Links to neuronal activity and vasomotion

Accurate glymphatic modeling almost certainly requires considering neuronal activity. NREM slow waves, which consist of highly synchronized neuronal up and down states (Vyazovskiy and Harris, 2013), appear to regulate glymphatic function and correlate with glymphatic activity (Xie et al., 2013; Hablitz et al., 2019). Pharmacological enhancement of slow wave sleep, e.g., via $\alpha$2-adrenergic agonists, promote glymphatic brain delivery (Lilius et al., 2019), whereas long-term slow wave sleep promotion by sodium oxybate in mouse models of Parkinson's disease can reduce the accumulation of $\alpha$-synuclein and promote perivascular AQP4 expression (Morawska et al., 2021). Inversely, the disruption of slow waves causes A$\beta$ accumulation (Ju et al., 2017), detailing a likely causal relationship between sleep slow waves and glymphatic function. One mechanism that could explain the link is functional hyperemia: increased neuronal activity draws additional blood (Turner et al., 2020), causing arteries to expand and therefore displace CSF in the surrounding perivascular spaces. Changes in blood volume are of highest magnitude during sleep, when slow waves cause global, oscillatory changes in blood volume. Their magnitude might explain why glymphatic clearance is faster during NREM sleep than during wakefulness. In fact, one recent study observed that slow wave modulations were immediately followed by hemodynamic oscillations coupled to CSF flow in humans (Fultz et al., 2019). Another study found that increasing vasomotion in awake mice by offering visual stimulus caused increased solute clearance in the visual cortex (van Veluw et al., 2020). It is also important to note that neuronal activity, especially sleep dependent synchronized neuronal activity, is coupled to substantial transmembrane ion transport (Ding et al., 2016) that also might drive glymphatic flow directly, without vasomotion as intermediary. In any case, because synchronized neuronal activity

during NREM slow wave sleep is homeostatically regulated, increases in intensity as a function of prior sleep and wakefulness (Borbély et al., 2016), and shows distinct spatiotemporal spreading across the brain (Massimini et al., 2004; Kurth et al., 2017), it is intriguing to speculate that sleep could be actively directing cellular clearance toward relevant areas of the CNS.

## MODELING

Having introduced some key mechanisms known or hypothesized to be at play in the glymphatic system, we now review existing models of those mechanisms. This section is organized parallel to Section Mechanisms, with subsections focused on flow in PVSs, transport in brain parenchyma, links between PVSs and parenchyma, brain efflux routes, and links to neuronal activity. We then discuss rOMT, which may go far to inform glymphatic models. This section closes with a few comments on the inherent utility and limits of modeling, and the modeling approaches that seem most productive for advancing the field.

### Perivascular flow

As discussed in Section Perivascular flow, a large number of possible drivers and modulators could affect perivascular flow and therefore deserve to be modeled. Among the mechanisms are perivascular pumping, functional hyperemia driven by neural activity, and osmotic effects.

Several papers have investigated perivascular pumping in idealized and localized geometries. An early model studied how CSF-filled cavities associated with syringomyelia formed in the spinal cord because of peristaltic pumping (Bilston et al., 2003). However, the wavelength of the vascular deformation was unreasonably short, and although the wavelength has not been measured, it is generally assumed to be in the range 20 cm to a couple of meters (Martinac and Bilston, 2019; Thomas, 2019; Daversin-Catty et al., 2020). Later, a pumping mechanism was proposed to be the offset between the cardiac and CSF pulsation, but this was deemed unlikely in (Martinac et al., 2021). Another early model asked how perivascular pumping might transport proteins in the direction antiparallel to blood, and hypothesized that surface chemistry could provide a valve-like effect for amyloid beta transport (Schley et al., 2006). The fluid motions (as opposed to amyloid motions) predicted by that model, however, are similar to those predicted by others, proceeding parallel to blood, on average, in most cases. Motivated by the model of Bilston et al. (Bilston et al. (2003), Wang and Olbricht (Wang and Olbricht, 2011) derived an analytical model of perivascular flow capable of explaining both influx and efflux, depending on the parameters in use. Their model predicts velocities around 20 $\mu$m/s, as seen *in vivo* (Mestre et al., 2018a; Bedussi et al., 2018), in reasonably sized perivascular spaces (Thomas, 2019). Still, the model involves simplifying assumptions: a circular cross-section, a sinusoidal wave pattern, and a very long annulus. Elliptical cross-sections observed *in vivo* reduce the resistance to flow and may constitute an evolutionary adaptation (Tithof et al., 2019). Yokoyama et al. (Yokoyama et al. (2021) observed that the ratio of wave amplitude to wavelength must be $\sim 10^{-4}$ in order to produce flows at 20 $\mu$m/s without a net pressure gradient. Localized computational studies have produced similar insights (Kedarasetti et al., 2020b; Daversin-Catty et al., 2020).

Boundary conditions should be considered carefully when modeling flows in perivascular spaces. If the surrounding tissue is soft enough to be deformed significantly when artery walls dilate or contract, we expect its deformation to remove kinetic energy from CSF and thereby reduce the flow speed. Kedarasetti et al. (2020a) imaged fluorescent neurons near a penetrating perivascular space, finding that the neurons moved in concert with artery walls, then went on to show slower flows in simulations with soft outer boundaries. However, other groups have observed no significant deformation (Mestre et al., 2020a), so further *in vivo* measurements are warranted.

There are other considerations in addition to side boundaries. Prior studies modeling perivascular spaces have frequently used periodic end boundaries (Wang and Olbricht, 2011) or zero-pressure end boundaries, which neglect effects of the fluid pathway beyond the modeling domain, such as resistance and compliance. Including them can change predictions significantly (Ladrón-de Guevara et al., 2020). The length of the modeling domain is also important. In perivascular pumping, the net flow direction is set by the travel direction of artery wall deformations. Therefore, in the limit of a domain that is infinitesimally short compared to the deformation wavelength, where the entire wall would deform simultaneously, perivascular pumping could produce no net flow. Although models have agreed closely with *in vivo* flow measurements (Mestre et al., 2018a), typical segments of real perivascular networks are shorter than a cardiac pulsation wavelength by a factor of $\sim 10^4$, bringing the mechanism into question. Daversin-Catty et al.

(Daversin-Catty et al. (2020) simulated shorter domains, finding much slower flows, and suggested that pulsation is accompanied by a small ($\approx 10^{-2}$ mmHg/cm) and steady pressure gradient of uncertain origin.

Recent studies have asked whether CSF flow in perivascular spaces could be driven by functional hyperemia, the local variation of blood volume in response to neuronal activity. Kedarasetti et al. (2020a) simulated slow, large artery dilations as expected during functional hyperemia, finding significant displacement of CSF. With additional simulations, Kedarasetti et al. (2021) found that functional hyperemia drove more periarterial flow than cardiac pulsation, in part because vasodilations associated with functional hyperemia have less temporal symmetry than those associated with cardiac pulsation. However, functional hyperemia typically propagates antiparallel to blood flow (Tian et al., 2010; Rungta et al., 2018) and would drive CSF in the same direction, if it imposes any net flow direction at all, but *in vivo* observations of CSF in perivascular spaces almost always show it moving parallel to blood. Also, although glymphatic transport occurs primarily during sleep, functional hyperemia is stronger during wakefulness (Turner et al., 2020). Further studies are required and should consider not only functional hyperemia, but also vasomotion linked to autonomic activity (Gu et al., 2022).

A few studies have argued that purely oscillatory flow, without net motion of fluid over time, could produce the rapid transport observed in experiments because of Taylor dispersion (Asgari et al., 2016; Smith and Verkman, 2018; Kedarasetti et al., 2020b; Faghih and Keith Sharp, 2021; Rey and Sarntinoranont, 2018). Taylor dispersion (also called shear-enhanced dispersion) occurs when shear in a narrow channel, such as a PVS, spreads solute along the channel axis whereas diffusion spreads solute laterally, resulting in greater effective axial diffusivity. However, recent theoretical arguments (Thomas, 2019) and numerical simulations (Troyetsky et al., 2021) concluded that Taylor dispersion in PVSs could speed transport only slightly, and much less than even weak net flows, resulting in far slower transport than those observed *in vivo*.

Most studies of perivascular spaces have avoided the complexities of bifurcations and of interactions among the many PVS segments that comprise the glymphatic system. Although the computational costs of simulating those complexities are daunting, flow and transport are surely affected by bifurcations and interactions, which are routinely simulated in studies of blood flow (e.g., see Goirand et al. (Goirand et al. (2021)). Daversin-Catty et al. (2020) simulated flow in a bifurcation, concluding that *in vivo* flow characteristics could most easily be reproduced via a combination of arterial pulsation and a steady pressure gradient of unknown source. Many studies have likewise pointed out that a small pressure gradient could drive the observed mean flows, but testable hypotheses about the source of that gradient are less common — and are an important topic for future work. Daversin-Catty et al. (Daversin-Catty et al. (2021) demonstrated that flow in bifurcations could be predicted with reasonable accuracy and substantially lower computational cost by solving the mass and Navier-Stokes equations in a single spatial dimension, by averaging radially and azimuthally. Coenen et al. (Coenen et al. (2021) produced analytic approximations for flow in non-axisymmetric annuli and suggested methods for solving PVS networks using those approximations, which are promising because they would be computationally feasible even for large networks. Interactions among segments have also been captured in hydraulic network models (Mestre et al., 2020a; Rey and Sarntinoranont, 2018; Faghih and Sharp, 2018; Tithof et al., 2022), discussed further below.

## Transport in brain parenchyma

Because of the tortuous and complex shape of the ECS, brain parenchyma is typically modeled as an unconsolidated porous medium. Numerical studies have often made the simplifying assumption that diffusion alone can predict solute motion. Such studies simulated random walks of individual molecules repeatedly (a Monte Carlo method), often using the MCell software package (Tao and Nicholson, 2004; Hrabe et al., 2004), making predictions that can be compared directly to RTI measurements. The typical tortuosity measured *in vivo*, $\lambda = 1.6$, is higher than that expected for simple diffusion around uniformly spaced convex objects, such as cell bodies or dendrites (Tao and Nicholson, 2004; Hrabe et al., 2004; Nicholson and Kamali-Zare, 2020). The discrepancy can be explained partially, but not completely, by interstitial viscosity (Zheng et al., 2017). However, adding dead spaces to the ECS has reproduced $\lambda = 1.6$ in Monte Carlo models (Hrabe et al., 2004; Tao et al., 2005; Nicholson, 2018). Dead spaces are local enlargements of the ECS, where diffusing molecules spend extra time, causing delays that increase the tortuosity $\lambda$ (see Section Mechanisms). Dead spaces have been visualized in living organotypic brain slices (Tønnesen et al., 2018) and inferred from diffusion measurements with carbon nanotubes (Godin et al., 2017; Nägerl et al., 2008). There is also other experimental evidence (Hrabetová et al., 2003). Combining three-dimensional electron microscopy data with

MCell showed that the ECS consisted of "tunnels" and "sheets" (Kinney et al., 2013), again implying a non-uniform ECS containing dead-spaces.

Some models of the parenchyma have also considered flow and advection effects. Again taking the tissue to be a porous medium, they typically model flow dynamics with Darcy's equation. Holter et al. (Holter et al., 2017), using a three-dimensional geometry of the neuropil based on (Kinney et al., 2013), predicted that advective transport could indeed be neglected with good accuracy, as long as ample flow in perivascular spaces maintains steep concentration gradients in the parenchyma. The same study found that the relative fraction of tunnels and sheets did not significantly affect the extracellular diffusion process. Ray et al. (Ray et al. (2019) found that RTI measurements might be explained more accurately by accounting for advection (see Section Mechanisms). Linninger et al. (Linninger et al. (2008) simulated parenchymal drug delivery, finding that using the injection to drive a flow caused penetration depths greater by a factor of 15 than with diffusion alone. Schreder et al. (Schreder et al. (2022) asked how parenchymal resistance depends on the spacing and arrangement of penetrating blood vessels, finding that, when considering regions large enough to contain many vessels, the per-arteriole conductance is approximately constant. Altogether, the role of advection in transport through brain parenchyma, during physiological conditions, pathological conditions, or clinical interventions, remains a topic of ongoing study.

Thomas (Thomas (2022) modeled effects on solute transport in the parenchyma caused when its porosity increases during the transition from wake to sleep (Xie et al., 2013). Greater porosity implies larger ECS spaces with lower hydraulic resistance, allowing more flow and stronger advection. Meanwhile, because enlarged ECS spaces are filled with fluid ejected from astrocytes and therefore low in substances like amyloid beta, solutes would be diluted in the ECS, weakening diffusion. Although the model is idealized, its prediction of strengthened advection and weakened diffusion is consistent with the simulation results of Jin et al. (Jin et al. (2016). Thus, observations that transport is stronger during sleep or sleep-like states than during wakefulness or wake-like states (Xie et al., 2013; Hablitz et al., 2019, 2020) suggest that advection plays an important role. If diffusion alone transported solutes from the deep brain to the cortical surface, concentrations would vary spatially to an unrealistic degree.

### Interfaces to perivascular spaces

The mechanisms that control influx at interfaces between PVSs and other fluid compartments are not well understood and are ripe for future modeling, although we will not discuss them further here. Mechanisms at the interfaces between perivascular spaces and parenchyma, on the other hand, have been an active topic of recent modeling.

It has been suggested that CSF might not leave perivascular spaces at all, with periarterial spaces connecting to perivenous spaces via pericapillary spaces. However, when Tithof et al. (Tithof et al. (2022) allowed for this pathway in a brain-wide hydraulic network model, they found flow there to be negligible for reasonable parameter values. Asgari et al. (Asgari et al. (2015) estimated the hydraulic resistances of two alternate pathways — one through AQP4 and astrocyte cell bodies, another through endfoot gaps — concluding that a large fraction of the water flow is intracellular because of the high AQP4 concentration and small gap size. *In vivo* gap size, however, is not known precisely. A further difficulty of this conclusion is that AQP4 admits only water molecules, prohibiting waste or nutrient transport through cell bodies.

Models have often focused on the pathway through endfoot gaps, and consequently, the arrangement and properties of astrocytes and their endfeet. Wang et al., 2021) observed that endfeet surrounding smaller vessels are themselves smaller, implying greater gap length per unit interface area. Continuing, the authors simulated flow through a network of PVSs and gaps modeled on images from super-resolution microscopy, finding that the observed variation in endfoot size allowed flow from PVSs to parenchyma to be more uniform than it otherwise would have been. That result is consistent with the conclusions of Romanò et al. (Romanò et al., 2020), who found PVS flows to depend sensitively on the porosity of the parenchyma at its interfaces with PVSs. Kedarasetti et al. (2021) modeled the parenchyma around periarterial spaces as a poro-elastic medium, that is, a porous medium in which the solid phase (here, cells and other tissue) is soft enough to be deformed appreciably by the flow of fluid through pores. The authors found that poro-elasticity acted like a rectifier, favoring flow into the parenchyma, and therefore parallel to blood, over flow out of the parenchyma. Thus, poro-elasticity might answer a key question: what mechanism sets the glymphatic flow direction? However, at the interfaces between perivenous

spaces and parenchyma, the same mechanism would favor flow anti-parallel to blood, so further modeling is needed.

### Efflux routes

Few glymphatic modeling studies include efflux, and those typically account only for perivenous spaces. Asgari et al. (Asgari et al. (2016)) simulated transport from a periarterial space, through parenchyma, to a venous PVS, and characterized solute concentrations over time for different boundary conditions. Rey and Sarntinoranont (Rey and Sarntinoranont, 2018) devised a lumped parameter model of flow near one arteriole and one vein, finding that flow was purely oscillatory, but that conclusion is unsurprising because flow was driven using standing (not traveling) vasodilations; no mechanisms were simulated that favored flow in one direction over the other. Faghih and Sharp (Faghih and Sharp, 2018) modeled perivascular flow — including efflux through perivenous spaces — using idealized branching based on Murray's law. They found the total resistance of the perivenous tree ($1.75 \times 10^{-3}$ mmHg•min/mL) to be smaller than that of the periarterial tree by a factor of $10^3$. Tithof et al. (2022) performed lumped parameter simulations to investigate uncertain parameters; they modeled the entire glymphatic CSF efflux as a single resistor with negligible resistance, based on the finding of Faghih and Sharp (Faghih and Sharp, 2018).

Some studies have explored glymphatic efflux in more detail. Vinje et al. (2021) concluded from solute transport simulations that tracer moves faster through pial periarterial than in perivenous spaces, which may explain experimental observations without the need for parenchymal flow. However, that conclusion depends strongly on the applied pressure differences, which were chosen to be identical for periarterial and perivenous spaces, although their values *in vivo* are unknown. Vardakis et al. (Vardakis et al. (2020)) devised a novel brain-wide finite element model with six transport compartments, accounting for perivenous efflux. Davoodi-Bojd et al. (Davoodi-Bojd et al., 2019) analyzed MRI measurements using two-compartment models for each of a collection of brain regions, finding that tracer transport was different in a rat model of diabetes than in wild-type rats. Elkin et al. (2018) implemented an OMT-based approach and identified differences in glymphatic transport — including efflux to lymphatic vessels — for rats under two different anesthetics (see Section Quantifying and defining glymphatic transport with optimal mass transport for an in-depth discussion of OMT). Vinje et al. (Vinje et al. (2020)) developed a compartmental model and demonstrated that elevated ICP may alter the proportion of CSF that exits the subarachnoid space via different efflux routes (including the glymphatic pathway with perivenous spaces). However, that conclusion follows directly from the authors' specification of a pressure-dependent compliance that varies inversely with ICP, which may require further validation.

Ample opportunities remain for exploring glymphatic efflux via computational approaches. Future studies should explore the relative proportion of fluid efflux via perivenous spaces versus white matter tracts; no models of the latter route exist, to the best of our knowledge. Modeling may also provide important evidence for the role of respiration as a glymphatic driving mechanism in perivenous spaces (Abbott, 2004; Kiviniemi et al., 2016; Santisakultarm et al., 2012) and CSF in general (Vinje et al., 2019; Helakari et al., 2022). Finally, future experimental studies could help illuminate whether there is direct efflux from the glymphatic system to the meningeal lymphatics; if so, techniques developed for modeling peripheral lymphatic vessels (Moore and Bertram, 2018; Margaris and Black, 2012) can be adapted to investigate glymphatic-lymphatic efflux.

### Links to neuronal activity and vasomotion

Although many models have been developed for the hemodynamic link between neuronal activity and local blood volume, often with application to functional MRI (Polimeni and Lewis, 2021), there is a lack of models explicitly linking neuronal activity to CSF flow in physiological conditions. Existing models that are closely related are those that predict CSF flow driven by spreading depolarization during ischemic stroke (Mestre et al., 2020a) and cardiac arrest (Du et al., 2022).

Models linking neuronal activity and vasomotion to CSF flow in physiological conditions are an important topic for future work. The link acts on millisecond timescales and can be understood as one sort of dynamic effect that changes over time and affects the perivascular transport network. Dynamic effects can influence connectivity and thickness of vessels, affecting local and global resistance to flow (Gross and Blasius, 2008; Porter and Gleeson, 2016; Martens and Klemm, 2017; Hu and Cai, 2013). Other dynamic effects take place over other timescales, including vascular remodeling in disease (weeks to months) (Jacobsen et al., 2009),

circadian rhythms (hours) (Hablitz et al., 2020), and vasomotion (seconds) (Carmignoto and Gómez-Gonzalo, 2010). Vasomotion has been modeled as local response mechanism in smooth muscle cells (Jacobsen et al., 2008), but also as the coupling of smooth muscle cells leading to electric signals propagating along vessel walls (Jacobsen et al., 2007; Hald et al., 2014). Alternating vessel responses due to cerebral autoregulation may even induce pressure gradients, leading to pumping across the network.

## Quantifying and defining glymphatic transport with optimal mass transport

In the glymphatic model, perivascular CSF transports solutes and clears wastes from brain tissue. However, the presence of bulk flow (i.e., advection) in neuropil is uncertain, as discussed in Section Mechanisms. Recent work has addressed the relative importance of advective and diffusive transport via data-driven methods, in which measurements (often from MRI) are combined with a mathematical model in order to make inferences about quantities that cannot be measured directly, such as fluid velocity (Koundal et al., 2020; Valnes et al., 2020; Elkin et al., 2018; Ray et al., 2021; Chen et al., 2022). To illustrate the requirements and capabilities of data-driven methods, we will discuss one in more detail: regularized optimal mass transport (rOMT). Given noisy, uncertain data — for example, dynamic contrast enhanced MRI (DCE-MRI) measurements — the rOMT algorithm determines the lowest-energy flow that could carry tracer from its initial spatial distribution to its final spatial distribution, subject to the constraint that the flow velocity and tracer concentrations satisfy the advection-diffusion equation. The resulting lowest-energy flow is an estimate of the fluid velocity as it varies through space and time. Knowing that velocity is useful because it allows one to quantify the relative importance of advection and diffusion in the observed tracer transport via its Péclet number, which may likewise vary over space and time. In addition, knowing the velocity allows predicting transport and the Péclet number for any other solute whose diffusivity is known, including endogenous proteins like amyloid beta and tau, which are difficult to isolate but have profound implications for neurodegeneration. rOMT also has potential for improving image registration (Elkin et al., 2018).

In recent work, rOMT revealed that solute speed is faster in CSF than in gray or white matter (Koundal et al., 2020; Elkin et al., 2018) and found two-fold differences in regional solute speed within the brain, which might imply varying importance of advection and diffusion across brain regions. These results suggest that advective transport dominates in CSF whereas diffusion and advection both contribute to glymphatic transport in the parenchyma. The analytical framework of rOMT provides novel insights in the local dynamics of glymphatic transport that may have implications for understanding pathophysiology of neurodegenerative diseases. Chen et al. (Chen et al. (2022) used rOMT and other tools to conclude that, in a rat model of cerebral amyloid angiopathy, compared to wild-type rats, flow and solute transport through brain tissue are significantly decreased, efflux along neck arteries is delayed, and efflux to the olfactory bulb is accelerated. The implication is that both glymphatic transport and lymphatic drainage are impaired and could be targets for future clinical interventions (Table 1)

## Key points to remember when modeling

Happily, mathematical modeling has proved to be "unreasonably effective" in a wide variety of physical and biological systems1. Still, neither the practice of modeling nor any single model is a panacea, and the glymphatic system — in which many material properties are inaccurately known, mechanisms interact, and novel phenomena emerge collectively — poses a substantial challenge. Thus, we encourage ongoing and expanded modeling efforts while also urging caution and rigor. Great models are built on stated hypotheses, make falsifiable clinical predictions, and are open to future improvements. Great models, although necessarily less realistic than *in vivo* observations, are a crucial complement because they allow counterfactuals to be tested and thereby raise new questions for future experiments. To enable this virtuous cycle, models should be presented with their assumptions and range of applicability stated as clearly as possible; some models apply more broadly than first expected, but many apply more narrowly than initially perceived. With models as with any scientific inquiry, we urge that results and data be distinguished from conclusions and interpretations, which are and should be more speculative. Categorizing existing models can help not only to organize prior results but also to reveal opportunities for impactful future studies. With Table 2, we attempt to do so.

Many mathematical models have been and will continue to be devised for mice, rats, and other animals, although human clinical applications are usually the ultimate goal. Translating models from other brains to human brains therefore requires careful consideration. Scaling laws based on dimensionless parameters like the Péclet number can help guide our intuition about how biophysical mechanisms vary with physical

**Table 1. Acronyms used in this paper**

| Acronym | Meaning |
|---|---|
| AQP4 | aquaporin-4 |
| BBB | blood-brain barrier |
| BOLD | blood-oxygen-level-dependent |
| CAA | cerebral amyloid angiopathy |
| CNS | central nervous system |
| CSF | cerebrospinal fluid |
| CT | computed tomography |
| DCE | dynamic contrast-enhanced |
| ECS | extracellular space |
| ICP | intracranial pressure |
| IOI | integrative optical imaging |
| IPAD | intramural periarterial drainage |
| ISF | interstitial fluid |
| MRI | magnetic resonance imaging |
| NREM | non-rapid eye movement |
| PET | positron emission tomography |
| PVS | perivascular space |
| rOMT | regularized optimal mass transport |
| RTI | real time iontophoresis |
| SAS | subarachnoid space |
| SB | Schrödinger bridge |
| SD | spreading depolarization |
| SLML | single-molecule localization microscopy |
| SPECT | single-photon emission computed tomography |
| STED | stimulated emission depletion |
| SUSHI | super-resolution shadow imaging |
| VCID | vascular contribution to cognitive impairment and dementia |

and geometrical constraints (Thomas, 2022; West et al., 1997). That said, humans are set apart from rodents by more than just their size. Body posture, sleep patterns, and cortical arteriole-to-venule ratio all differ significantly and seem relevant to the glymphatic system. Gyrencephalic (folded) and lissencephalic (smooth) brains may host substantially different glymphatic systems. Even small-scale biochemistry could vary. Successful translation from rodents to humans will require models cognizant of these and other considerations.

## USE CASE: DRUG DELIVERY

Neurobiology is often beautiful, but we aspire to make models that are practical, as well. As an example of one practical, clinical application, we consider in this section one use case: delivery of drugs directly to the CNS, unimpeded by the BBB, via CSF flow in the glymphatic system.

Delivery of drugs and diagnostic agents to the CNS is particularly difficult because of the BBB that protects the CNS from exogenous substances by both passive and active mechanisms, requiring that intravenously or orally administered CNS-targeted drugs be given in excessive doses that often cause adverse systemic effects. Several noninvasive and invasive techniques have been utilized to overcome the BBB (Terstappen et al., 2021). Of the invasive procedures, direct administration to the CSF allows therapeutics to bypass the BBB endothelium. In particular, the lumbar intrathecal route (Kevin et al., 2018) is used widely to deliver small-molecule drugs, and also larger therapeutics such as polypeptides (Staats et al., 2004), proteins

**Table 2. Many models have been developed, with application to different parts of the glymphatic system, and using different modeling approaches, with strengths and limitations varying accordingly**

| Perivascular flow | | | |
|---|---|---|---|
| *Type* | *Strengths* | *Limitations* | *Examples* |
| Lubrication theory | Analytic approach makes scaling clear. | Highly idealized geometry. Single mechanism. | (Wang and Olbricht, 2011; Coenen et al., 2021; Bilston et al., 2003; Schley et al., 2006) |
| Numerical Navier-Stokes solution, 2D or 3D | Applicable to complicated geometry. | Prohibitively expensive if PVS length and cardiac wave speeds are realistic. Bifurcations studied only rarely; networks currently too expensive. | (Kedarasetti et al., 2020b; Daversin-Catty et al., 2020; Kedarasetti et al., 2020a; Yokoyama et al., 2021; Vinje et al., 2021) |
| Numerical Navier-Stokes solution, 1D | Low computational cost accommodates whole PVS networks. | Neglects sometimes-important details like PVS shape. | (Daversin-Catty et al., 2021) |
| Numerical advection-diffusion solution | Predict solute transport. | Requires knowledge of velocity fields. Highly idealized or prohibitively expensive. | (Keith Sharp et al., 2019; Troyetsky et al., 2021) |
| Hydraulic resistance modeling | Inexpensive calculations can inform brain-wide models. | Idealized: typically assumes parallel, steady flow and simple geometry. | (Tithof et al., 2019; Rey and Sarntinoranont, 2018; Faghih and Sharp, 2018) |
| **Transport in brain parenchyma** | | | |
| *Type* | *Strengths* | *Limitations* | *Examples* |
| Monte Carlo molecular random walks | Direct calculation of porosity, tortuosity, and effective diffusivity from microscale ECS geometry | Requires knowledge of microscale geometry. Prohibitively expensive for large regions. | (Tao and Nicholson, 2004; Hrabe et al., 2004; Nicholson and Kamali-Zare, 2020; Tao et al., 2005; Nicholson, 2018; Kinney et al., 2013) |
| Numerical advection-diffusion solution | Predict transport via flow and diffusion | Required inputs (e.g., permeability, porosity, tortuosity) often poorly characterized or derived from measurements subject to fixation artifacts. | (Ray et al., 2019; Asgari et al., 2016; Holter et al., 2017) |
| Analytic advection solution | Predict flow | Required inputs (e.g., permeability, porosity, tortuosity) often poorly characterized or derived from measurements subject to fixation artifacts. | (Schreder et al., 2022) |
| **Interfaces to perivascular spaces** | | | |
| *Type* | *Strengths* | *Limitations* | *Examples* |
| Numerical Navier-Stokes solution with porous boundaries | Pioneering models of PVS-parenchyma interface. | Tissue properties poorly characterized. Expensive, depending on PVS flow parameters. Networks currently too expensive. | (Kedarasetti et al., 2021; Wang et al., 2021; Romanò et al., 2020) |
| **Efflux routes** | | | |
| *Type* | *Strengths* | *Limitations* | *Examples* |
| Hydraulic network models | Based on hypothesized flow mechanisms. Can span brain-wide, incorporate efflux. Computationally inexpensive. | Many simplifications, many poorly-characterized parameters. No solute transport. | (Mestre et al., 2020a; Asgari et al., 2015; Rey and Sarntinoranont, 2018; Faghih and Sharp, 2018; Tithof et al., 2022) |

(*Continued on next page*)

**Table 2. *Continued***

| | | | |
|---|---|---|---|
| Perivascular flow | | | |
| Compartment models | Easily compared to *in vivo* clearance measurements. Can span brain-wide, incorporate efflux. Less computationally expensive than most other techniques. | Many simplifications, many poorly-characterized parameters, flow mechanisms stated less explicitly. | (Vardakis et al., 2020) |
| Links to neuronal activity | | | |
| *Type* | *Strengths* | *Limitations* | *Examples* |
| Numerical continuity solution, with artery constriction set by spreading depolarization | Pioneering models of links to neuronal activity | Applied only to pathological cases of stroke and cardiac arrest. Neglect drivers other than constriction. | (Mestre et al., 2020a; Du et al., 2022) |

(Schulz et al., 2018), oligonucleotides (Finkel et al., 2017), and diagnostic agents such as gadolinium-labeled (Ringstad et al., 2018) and radionuclide-labeled (Verma et al., 2020) CSF tracers. However, the slow diffusion rate of large solutes from the subarachnoid CSF to deep CNS structures restricts the efficacy and utility of intrathecal therapeutics (Wolak and Thorne, 2013). For example, a recent study of intrathecal administration of iron-based nanoparticles (Venugopal et al., 2017) found uptake into the parenchyma occurring mainly near perivascular spaces, not across the cortical surface elsewhere. Advective glymphatic CSF influx in periarterial spaces could be harnessed to deliver intrathecal therapeutics widely to the deep CNS structures.

In clinical practice, intrathecal drugs are usually administered at the outpatient clinic in the awake state, when the glymphatic system is nearly inactive. Enhanced glymphatic flow facilitated by deep sleep or other interventions enhancing glymphatic CSF influx could theoretically improve drug delivery to the brain and spinal cord parenchymas. Preclinical rodent studies have found that dexmedetomidine, a clinically used $\alpha_2$-adrenergic agonist sedative that enhances both glymphatic influx and efflux (Benveniste et al., 2017), increased the brain and spinal cord exposure to intracisternally administered small-molecular opioids oxycodone and naloxone and increases the delivery of an IgG-sized amyloid-beta antibody to the rat brain (Lilius et al., 2019). Whereas dexmedetomidine-induced controlled sedation mimics NREM sleep, another clinically intriguing option to transiently enhance periarterial CSF influx without affecting consciousness is the systemic administration of hypertonic solutions. Systemic hyperosmolality leads to movement of water from the CNS to peripheral circulation, replaced by rapid influx of CSF from the subarachnoid space, possibly driven by the osmotic pressure gradient (Buishas et al., 2014; Linninger et al., 2017). In a study in mice, hypertonicity induced by intraperitoneal mannitol or hypertonic saline enhanced the penetration of intracisternally infused IgG-sized amyloid-beta antibody to the brain and its binding to amyloid-beta plaques manifold (Plog et al., 2018). The results suggest not only that hypertonicity could be used to enhance drug delivery, but also that solutes in the extracellular space are transported, at least in part, by advection, because diffusive transport would typically decrease after water moves from brain cells to ECS (Thomas, 2022). In rats, systemic hypertonic saline enhanced the delivery of morphine to the spinal cord after lumbar intrathecal administration, resulting in enhanced antinociception (Blomqvist et al., 2022).

Although there are several suitable potential interventions available for glymphatic-enhanced drug delivery, they have not yet been tested in randomized controlled clinical trials. Recent work by Eide et al. has highlighted the possibility for modeling studies to measure CSF clearance with very limited data. The small-molecule MRI contrast agent gadobutrol — sharing properties with typical CNS-targeted drugs such as low BBB permeability — was infused intrathecally, and its CNS distribution over time was assessed using MRI in different patient populations (Ringstad et al., 2018). Eide et al. measured gadobutrol concentrations in the systemic circulation and used pharmacokinetic models (also known as compartment models or control volume models) to estimate clearance of the intrathecally administered tracer (Eide et al., 2021a). Because repeated blood sampling is readily available in the clinic, pharmacokinetic modeling could provide rough estimates of efficacy of CNS delivery. Drug-specific clearance is typically assessed with multimodal imaging studies (Tangen et al., 2020). The Linninger lab has developed a framework to combine dynamic imaging data with detailed modeling of CSF dynamics (Tangen et al., 2017) to predict biodispersion to target spinal or cerebral delivery sites and clearance routes as a function of infusion setting. Future work

will define the optimal characteristics of drugs to be delivered through CSF administration possibly aided by the glymphatic pathway and the potential clinical utility of this delivery route.

## OUTLOOK AND FUTURE WORK

Recent modeling of CSF / ISF flow and solute transport in the brain has produced discoveries and insights which are often subjects of widespread consensus. Meanwhile, controversies continue, and although some can be resolved with existing knowledge, others point helpfully to important future work.

### Perivascular flow

The mechanisms that drive flow, especially in perivascular spaces, still deserve further study. Models of vasoconstriction caused by spreading depolarization can reproduce flows and transport observed during stroke and cardiac arrest, but in physiological situations, the story is less clear. Arterial pulsation with the cardiac cycle induces CSF oscillations and increases effective diffusivity modestly; whether it also drives net flow is debated. Many researchers have noted that net flow could be driven by a small, steady pressure gradient, but few mechanisms have been suggested for maintaining such a gradient. (Artifactual gradients from tracer injection do not seem to explain the observed flows (Raghunandan et al., 2021).) The idea is fraught: both influx and efflux routes connect to the subarachnoid space, so a pressure difference between parenchyma and subarachnoid space (SAS) would not alone cause circulation. Future experiments might explore whether the SAS is segregated into influx and efflux regions. Experiments should also determine the stiffness of tissue around pial and penetrating perivascular spaces, which is currently debated and affects models greatly; acoustic methods hold promise. Future models might make progress by considering PVSs of realistic lengths and accounting for interactions of multiple PVSs segments, with careful attention to bifurcations, boundary conditions and dynamic interactions.

Functional hyperemia almost certainly plays an important role in perivascular flows but is unlikely to be the sole driver, because flow has been observed in experiments where the slow, large-amplitude vasomotion characteristic of functional hyperemia was absent, particularly during anesthesia (Hablitz et al., 2019). Future experiments and models could quantify the effects of functional hyperemia, characterize its variation with brain state, and determine whether low-frequency flows in SAS and ventricles link to PVSs, as suggested by a recent anatomical study (Magdoom et al., 2019). Experiments might also determine the porosity and permeability of penetrating perivascular spaces, which are essentially unknown and have profound implications for model predictions.

### Transport in brain parenchyma

In brain parenchyma, solute transport almost certainly occurs via both diffusion and advection, with diffusion likely making the greater contribution, except possibly for large solutes (e.g., tau). The relative importance of diffusion and advection vary spatially and with brain state. Some fluid flow through the parenchyma is implied by the model of glymphatic circulation; flow closes the circuit, because fluid must be conserved. That flow may pass through the extracellular space, through astrocyte bodies, and/or through pericapillary spaces (if they exist). Besides completing the circuit, that flow would also maintain the concentration gradients necessary for diffusive transport. Future experiments could reveal much about transport and flow in the parenchyma by determining the permeability of the extracellular space, the magnitudes of solute concentration gradients, and whether or not pericapillary spaces exist. MRI, rOMT, and super-resolution *in vivo* imaging via carbon nanotubes all seem particularly promising.

### Interfaces to perivascular spaces

Interfaces between perivascular spaces and parenchyma are an important control site for the glymphatic system, as evidenced by flow modulation via the AQP4 that decorates endfeet at those interfaces. But the control mechanism is unknown, and future models should probe it. Poro-elasticity at that interface may play an important role, perhaps setting the circulation direction in lieu of valves. Future models should explore poro-elasticity further, and future experiments should measure tissue stiffness (see above). Interfaces between perivascular spaces and other fluid compartments control the origins and amounts of fluid in PVSs, setting flow rates, recirculation rates, and bypass rates. These effects, often osmotic, have been modeled little and warrant future study.

### Efflux routes

Efflux routes are poorly characterized. Models can make better efflux predictions only after experiments provide more ground truth. Mapping efflux routes is essential, although tricky because concentrations are smaller than in influx routes. Future experiments could reveal how efflux routes link to meningeal lymph vessels or other skull exits. Determining whether the SAS is segregated into influx and efflux regions is also important (see above). Because large tracer particles cannot access efflux routes, PET/SPECT, MRI, and perhaps light sheet microscopy are the most promising tools. Experiments would also do well to explore effects of respiration and the intrinsic pumping of lymph vessels. Brain-wide models (hydraulic networks, 1D simulations, and compartment models) can suggest which parameters most need measurement and make improved efflux predictions once measurements are done.

### Links to neuronal activity and vasomotion

Opportunities abound for modeling glymphatic links to neuronal activity, which has rarely been explored in the past. Slow wave activity and slow wave modulation both seem important and may influence flows directly or indirectly (via vasomotion / functional hyperemia). Future experiments can contribute by measuring neuronal activity, fluid flow, and vasomotion simultaneously, e.g., with two-photon imaging of GCaMP mice (which are genetically modified such that neuronal activity causes fluorescence).

## CONCLUSION

Many models have been developed for the mechanisms of the glymphatic system (Table 2). As these tools are expanded and refined, we urge that each be applied where most useful, with strengths and limitations made clear, and in combination with other models when necessary. Models are essential for their flexibility, tendency to produce new hypotheses, and capacity for testing counterfactuals that cannot be addressed in physiological conditions. Models must be validated experimentally — *in vivo* if possible — where discrepancies can lead to key insights. Open conversation is essential and can be facilitated through more workshops like the one that inspired this paper.

## AUTHOR CONTRIBUTIONS

All authors attended the workshop "The glymphatic system: From theoretical models to clinical applications," engaged in extended discussion, and wrote the paper collaboratively.

## DECLARATION OF INTERESTS

We declare no conflicts of interest.

## REFERENCES

Abbott, N.J., Pizzo, M.E., Preston, J.E., Janigro, D., and Thorne, R.G. (2018). The role of brain barriers in fluid movement in the cns: is there a 'glymphatic' system? Acta Neuropathol. *135*, 387–407.

Abbott, N.J. (2004). Evidence for bulk flow of brain interstitial fluid: significance for physiology and pathology. Neurochem. Int. *45*, 545–552. https://doi.org/10.1016/j.neuint.2003.11.006.

Achariyar, T.M., Li, B., Peng, W., Verghese, P.B., Shi, Y., McConnell, E., Benraiss, A., Kasper, T., Song, W., Takano, T., et al. (2016). Glymphatic distribution of CSF-derived apoE into brain is isoform specific and suppressed during sleep deprivation. Mol. Neurodegener. *11*, 74.

Agarwal, N., and Carare, R.O. (2020). Cerebral vessels: an overview of anatomy, physiology, and role in the drainage of fluids and solutes. Front. Neurol. *11*, 611485. https://doi.org/10.3389/fneur.2020.611485.

Ahn, J.H., Cho, H., Kim, J.H., Kim, S.H., Ham, J.S., Park, I., Suh, S.H., Hong, S.P., Song, J.H., Hong, Y.K., et al. (2019). Meningeal lymphatic vessels at the skull base drain cerebrospinal fluid. Nature *572*, 62–66. https://doi.org/10.1038/s41586-019-1419-5.

Albargothy, N.J., Johnston, D.A., MacGregor-Sharp, M., Weller, R.O., Verma, A., Hawkes, C.A., and Carare, R.O. (2018). Convective influx/glymphatic system: tracers injected into the CSF enter and leave the brain along separate periarterial basement membrane pathways. Acta Neuropathol. *136*, 139–152. https://doi.org/10.1007/s00401-018-1862-7.

Aldea, R., Weller, R.O., Wilcock, D.M., Carare, R.O., and Richardson, G. (2019). Cerebrovascular smooth muscle cells as the drivers of intramural periarterial drainage of the brain. Front. Aging Neurosci. *11*, 1.

Alshuhri, M.S., Gallagher, L., Work, L.M., and Holmes, W.M. (2021). Direct imaging of glymphatic transport using H217O MRI. JCI Insight *6*, 141159. https://doi.org/10.1172/jci.insight.141159.

Annadurai, N., De Sanctis, J.B., Hajdúch, M., and Das, V. (2021). Tau secretion and propagation: perspectives for potential preventive interventions in Alzheimer's disease and other tauopathies. Exp. Neurol. *343*, 113756. https://doi.org/10.1016/j.expneurol.2021.113756.

Arizono, M., Inavalli, V.V.G.K., Panatier, A., Pfeiffer, T., Angibaud, J., Levet, F., Ter Veer, M.J.T., Stobart, J., Bellocchio, L., Mikoshiba, K., et al. (2020). Structural basis of astrocytic Ca2+ signals at tripartite synapses. Nat. Commun. *11*, 1906. https://doi.org/10.1038/s41467-020-15648-4.

Asgari, M., de Zélicourt, D., and Kurtcuoglu, V. (2015). How astrocyte networks may contribute to cerebral metabolite clearence. Sci. Rep. *5*, 15024. https://doi.org/10.1038/srep15024.

Asgari, M., de Zélicourt, D., and Kurtcuoglu, V. (2016). Glymphatic solute transport does not require bulk flow. Sci. Rep. *6*, 38635–38711.

Aspelund, A., Antila, S., Proulx, S.T., Karlsen, T.V., Karaman, S., Detmar, M., Wiig, H., and Alitalo, K. (2015). A dural lymphatic vascular system that drains brain interstitial fluid and macromolecules. J. Exp. Med. *212*, 991–999. https://doi.org/10.1084/jem.20142290.

Bèchet, N.B., Kylkilahti, T.M., Mattsson, B., Petrasova, M., Shanbhag, N.C., and Lundgaard, I. (2020). Light sheet fluorescence microscopy of optically cleared brains for studying the glymphatic system. J. Cereb. Blood Flow Metab. *40*, 1975–1986. https://doi.org/10.1177/0271678X20924954.

Bèchet, N.B., Shanbhag, N.C., and Lundgaard, I. (2021). Glymphatic pathways in the gyrencephalic brain. J. Cereb. Blood Flow Metab. *41*, 2264–2279. https://doi.org/10.1177/0271678X21996175.

Bedussi, B., Van Der Wel, N.N., de Vos, J., van Veen, H., Siebes, M., Bakker, E.N., and VanBavel, E. (2017). Paravascular channels, cisterns, and the subarachnoid space in the rat brain: a single compartment with preferential pathways. J. Cereb. Blood Flow Metab. *37*, 1374–1385.

Bedussi, B., Almasian, M., de Vos, J., VanBavel, E., and Bakker, E.N. (2018). Paravascular spaces at the brain surface: low resistance pathways for cerebrospinal fluid flow. J. Cereb. Blood Flow Metab. *38*, 719–726.

Bellesi, M., de Vivo, L., Tononi, G., and Cirelli, C. (2015). Effects of sleep and wake on astrocytes: clues from molecular and ultrastructural studies. BMC Biol. *13*, 66.

Benveniste, H., and Nedergaard, M. (2022). Cerebral small vessel disease: a glymphopathy? Curr. Opin. Neurobiol. *72*, 15–21.

Benveniste, H., Lee, H., Ding, F., Sun, Q., Al-Bizri, E., Makaryus, R., Probst, S., Nedergaard, M., Stein, E.A., and Lu, H. (2017). Anesthesia with dexmedetomidine and low-dose isoflurane increases solute transport via the glymphatic pathway in rat brain when compared with high-dose isoflurane. Anesthesiology *127*, 976–988.

Benveniste, H., Heerdt, P.M., Fontes, M., Rothman, D.L., and Volkow, N.D. (2019a). Glymphatic system function in relation to anesthesia and sleep states. Anesth. Analg. *128*, 747–758.

Benveniste, H., Liu, X., Koundal, S., Sanggaard, S., Lee, H., and Wardlaw, J. (2019b). The glymphatic system and waste clearance with brain aging: a review. Gerontology *65*, 106–119.

Bernardi, G., Cecchetti, L., Siclari, F., Buchmann, A., Yu, X., Handjaras, G., Bellesi, M., Ricciardi, E., Kecskemeti, S.R., Riedner, B.A., et al. (2016). Sleep reverts changes in human gray and white matter caused by wake-dependent training. Neuroimage *129*, 367–377.

Bilston, L.E., Fletcher, D.F., Brodbelt, A.R., and Stoodley, M.A. (2003). Arterial pulsation-driven cerebrospinal fluid flow in the perivascular space: a computational model. Comput. Methods Biomech. Biomed. Engin. *6*, 235–241.

Blomqvist, K.J., Skogster, M.O.B., Kurkela, M.J., Rosenholm, M.P., Ahlström, F.H.G., Airavaara, M.T., Backman, J.T., Rauhala, P.V., Kalso, E.A., Lilius, T.O., and Lilius, T.O. (2022). Systemic hypertonic saline enhances glymphatic spinal cord delivery of lumbar intrathecal morphine. J. Control. Release *344*, 214–224.

Borbély, A.A., Daan, S., Wirz-Justice, A., and Deboer, T. (2016). The two-process model of sleep regulation: a reappraisal. J. Sleep Res. *25*, 131–143.

Borha, A., Chagnot, A., Goulay, R., Emery, E., Vivien, D., and Gaberel, T. (2020). Cranioplasty reverses dysfunction of the solutes distribution in the brain parenchyma after decompressive craniectomy. Neurosurgery *87*, 1064–1069.

Bradbury, M.W., and Cole, D.F. (1980). The role of the lymphatic system in drainage of cerebrospinal fluid and aqueous humour. J. Physiol. *299*, 353–365.

Brown, R., Benveniste, H., Black, S.E., Charpak, S., Dichgans, M., Joutel, A., Nedergaard, M., Smith, K.J., Zlokovic, B.V., and Wardlaw, J.M. (2018). Understanding the role of the perivascular space in cerebral small vessel disease. Cardiovasc. Res. *114*, 1462–1473.

Buishas, J., Gould, I.G., and Linninger, A.A. (2014). A computational model of cerebrospinal fluid production and reabsorption driven by starling forces. Croat. Med. J. *55*, 481–497.

Cai, X., Qiao, J., Kulkarni, P., Harding, I.C., Ebong, E., and Ferris, C.F. (2020). Imaging the effect of the circadian light-dark cycle on the glymphatic system in awake rats. Proc. Natl. Acad. Sci. USA *117*, 668–676.

Carare, R.O., Bernardes-Silva, M., Newman, T.A., Page, A.M., Nicoll, J.A.R., Perry, V.H., and Weller, R.O. (2008). Solutes, but not cells, drain from the brain parenchyma along basement membranes of capillaries and arteries: significance for cerebral amyloid angiopathy and neuroimmunology. Neuropathol. Appl. Neurobiol. *34*, 131–144.

Carmignoto, G., and Gómez-Gonzalo, M. (2010). The contribution of astrocyte signalling to neurovascular coupling. Brain Res. Rev. *63*, 138–148.

Carr, J.B., Thomas, J.H., Liu, J., and Shang, J.K. (2021). Peristaltic pumping in thin non-axisymmetric annular tubes. J. Fluid Mech. *917*, A10.

Chen, G.F., Xu, T.H., Yan, Y., Zhou, Y.R., Jiang, Y., Melcher, K., and Xu, H.E. (2017). Amyloid beta: structure, biology and structure-based therapeutic development. Acta Pharmacol. Sin. *38*, 1205–1235.

Chen, X., Liu, X., Koundal, S., Elkin, R., Zhu, X., Monte, B., Xu, F., Dai, F., Pedram, M., Lee, H., et al. (2022). Cerebral amyloid angiopathy is associated with glymphatic transport reduction and time-delayed solute drainage along the neck arteries. Nat. Aging *2*, 214–223.

Coenen, W., Zhang, X., and Sánchez, A. (2021). Lubrication analysis of peristaltic motion in non-axisymmetric annular tubes. J. Fluid Mech. *921*, R2.

Colbourn, R., Hrabe, J., Nicholson, C., Perkins, M., Goodman, J.H., and Hrabetova, S. (2021). Rapid volume pulsation of the extracellular space coincides with epileptiform activity in mice and depends on the NBCe1 transporter. J. Physiol. *599*, 3195–3220.

Coloma, M., Schaffer, J.D., Carare, R.O., Chiarot, P.R., and Huang, P. (2016). Pulsations with reflected boundary waves: a hydrodynamic reverse transport mechanism for perivascular drainage in the brain. J. Math. Biol. *73*, 469–490.

Coloma, M., Schaffer, J.D., Huang, P., and Chiarot, P.R. (2019). Boundary waves in a microfluidic device as a model for intramural periarterial drainage. Biomicrofluidics *13*, 024103–024112.

Constantinople, C.M., and Bruno, R.M. (2011). Effects and mechanisms of wakefulness on local cortical networks. Neuron *69*, 1061–1068.

Croci, M., Vinje, V., and Rognes, M.E. (2019). Uncertainty quantification of parenchymal tracer distribution using random diffusion and convective velocity fields. Fluids Barriers CNS *16*, 32.

Cserr, H.F., Cooper, D.N., Suri, P.K., and Patlak, C.S. (1981). Efflux of radiolabeled polyethylene glycols and albumin from rat brain. Am. J. Physiol. *240*, F319–F328.

Cserr, H.F. (1971). Physiology of the choroid plexus. Physiol. Rev. *51*, 273–311.

Cunningham, E.L., McGuinness, B., McAuley, D.F., Toombs, J., Mawhinney, T., O'Brien, S., Beverland, D., Schott, J.M., Lunn, M.P., Zetterberg, H., and Passmore, A.P. (2019). CSF beta-amyloid 1-42 concentration predicts delirium following elective arthroplasty surgery in an observational cohort study. Ann. Surg. *269*, 1200–1205.

Daversin-Catty, C., Vinje, V., Mardal, K.A., and Rognes, M.E. (2020). The mechanisms behind perivascular fluid flow. PLoS One *15*, e0244442–e0244520.

Daversin-Catty, C., Gjerde, I.G., and Rognes, M.E. (2021). Geometrically Reduced Modelling of Pulsatile Flow in Perivascular Networks.

Davoodi-Bojd, E., Ding, G., Zhang, L., Li, Q., Li, L., Chopp, M., Zhang, Z.G., and Jiang, Q. (2019). Modeling glymphatic system of the brain using mri. Neuroimage *188*, 616–627.

de Vivo, L., Bellesi, M., Marshall, W., Bushong, E.A., Ellisman, M.H., Tononi, G., and Cirelli, C. (2017). Ultrastructural evidence for synaptic scaling across the wake/sleep cycle. Science *355*, 507–510.

Demiral, Ş.B., Tomasi, D., Sarlls, J., Lee, H., Wiers, C.E., Zehra, A., Srivastava, T., Ke, K., Shokri-Kojori, E., Freeman, C.R., et al. (2019). Apparent diffusion coefficient changes in human brain during sleep – does it inform on the existence of a glymphatic system? Neuroimage *185*, 263–273.

Ding, F., O'Donnell, J., Xu, Q., Kang, N., Goldman, N., and Nedergaard, M. (2016). Changes in the composition of brain interstitial ions control the sleep-wake cycle. Science *352*, 550–555. https://doi.org/10.1126/science.aad4821.

Dreha-Kulaczewski, S., Joseph, A.A., Merboldt, K.D., Ludwig, H.C., Gärtner, J., and Frahm, J. (2015). Inspiration is the major regulator of human CSF flow. J. Neurosci. *35*, 2485–2491.

Dreha-Kulaczewski, S., Joseph, A.A., Merboldt, K.D., Ludwig, H.C., Gärtner, J., and Frahm, J. (2017). Identification of the upward movement of human CSF in vivo and its relation to the brain venous system. J. Neurosci. *37*, 2395–2402.

Du, T., Mestre, H., Kress, B.T., Liu, G., Sweeney, A.M., Samson, A.J., Rasmussen, M.K., Mortensen, K.N., Bork, P.A.R., Peng, W., et al. (2022). Cerebrospinal fluid is a significant fluid source for anoxic cerebral oedema. Brain *145*, 787–797.

Eide, P.K., and Ringstad, G. (2021). Cerebrospinal fluid egress to human parasagittal dura and the impact of sleep deprivation. Brain Res. *1771*, 147669.

Eide, P.K., Holm, S., and Sorteberg, W. (2012). Simultaneous monitoring of static and dynamic intracranial pressure parameters from two separate sensors in patients with cerebral bleeds: comparison of findings. Biomed. Eng. Online *11*, 66. https://doi.org/10.1186/1475-925X-11-66.

Eide, P.K., Vatnehol, S.A.S., Emblem, K.E., and Ringstad, G. (2018). Magnetic resonance imaging provides evidence of glymphatic drainage from human brain to cervical lymph nodes. Sci. Rep. *8*, 7194.

Eide, P.K., Mariussen, E., Uggerud, H., Pripp, A.H., Lashkarivand, A., Hassel, B., Christensen, H., Hovd, M.H., and Ringstad, G. (2021a). Clinical application of intrathecal gadobutrol for assessment of cerebrospinal fluid tracer clearance to blood. JCI insight *6*, 147063.

Eide, P.K., Valnes, L.M., Lindstrøm, E.K., Mardal, K.-A., and Ringstad, G. (2021b). Direction and magnitude of cerebrospinal fluid flow vary substantially across central nervous system diseases. Fluids Barriers CNS *18*, 16–18.

Eide, P.K., Vinje, V., Pripp, A.H., Mardal, K.A., and Ringstad, G. (2021c). Sleep deprivation impairs molecular clearance from the human brain. Brain *144*, 863–874.

Elkin, R., Nadeem, S., Haber, E., Steklova, K., Lee, H., Benveniste, H., and Allen, T. (2018). Glymphvis: visualizing glymphatic transport pathways using regularized optimal transport. In Medical Image Computing and Computer Assisted Intervention – MICCAI 2018, A.F. Frangi, J.A. Schnabel, C. Davatzikos, C. Alberola-López, and G. Fichtinger, eds. (Springer International Publishing), pp. 844–852.

Engelhardt, B., Carare, R.O., Bechmann, I., Flügel, A., Laman, J.D., and Weller, R.O. (2016). Vascular, glial, and lymphatic immune gateways of the central nervous system. Acta Neuropathol. *132*, 317–338.

Evans, P.G., Sokolska, M., Alves, A., Harrison, I.F., Ohene, Y., Nahavandi, P., Ismail, O., Miranda, E., Lythgoe, M.F., Thomas, D.L., and Wells, J.A. (2020). Non-invasive MRI of blood-cerebrospinal fluid barrier function. Nat. Commun. *11*, 2081.

Faghih, M.M., and Keith Sharp, M. (2021). Mechanisms of tracer transport in cerebral perivascular spaces. J. Biomech. *118*, 110278.

Faghih, M.M., and Sharp, M.K. (2018). Is bulk flow plausible in perivascular, paravascular and paravenous channels? Fluids Barriers CNS *15*, 17.

Fenstermacher, J., and Kaye, T. (1988). Drug "diffusion" within the brain. Ann. N. Y. Acad. Sci. *531*, 29–39.

Fenstermacher, J.D., and Patlak, C.S. (1976). The movements of water and solutes in the brains of mammals. In Dynamics of brain edema (Springer), pp. 87–94.

Ferris, C.F. (2021). Rethinking the conditions and mechanism for glymphatic clearance. Front. Neurosci. *15*, 624690.

Finkel, R.S., Mercuri, E., Darras, B.T., Connolly, A.M., Kuntz, N.L., Kirschner, J., Chiriboga, C.A., Saito, K., Servais, L., Tizzano, E., et al. (2017). Nusinersen versus sham control in infantile-onset spinal muscular atrophy. N. Engl. J. Med. *377*, 1723–1732.

Fultz, N.E., Bonmassar, G., Setsompop, K., Stickgold, R.A., Rosen, B.R., Polimeni, J.R., and Lewis, L.D. (2019). Coupled electrophysiological, hemodynamic, and cerebrospinal fluid oscillations in human sleep. Science *366*, 628–631.

Godin, A.G., Varela, J.A., Gao, Z., Danné, N., Dupuis, J.P., Lounis, B., Groc, L., and Cognet, L. (2017). Single-nanotube tracking reveals the nanoscale organization of the extracellular space in the live brain. Nat. Nanotechnol. *12*, 238–243.

Goedert, M., Eisenberg, D.S., and Crowther, R.A. (2017). Propagation of tau aggregates and neurodegeneration. Annu. Rev. Neurosci. *40*, 189–210.

Goirand, F., Le Borgne, T., and Lorthois, S. (2021). Network-driven anomalous transport is a fundamental component of brain microvascular dysfunction. Nat. Commun. *12*, 7295.

Goulay, R., Flament, J., Gauberti, M., Naveau, M., Pasquet, N., Gakuba, C., Emery, E., Hantraye, P., Vivien, D., Aron-Badin, R., and Gaberel, T. (2017). Subarachnoid hemorrhage severely impairs brain parenchymal cerebrospinal fluid circulation in nonhuman primate. Stroke *48*, 2301–2305.

Gross, T., and Blasius, B. (2008). Adaptive coevolutionary networks: a review. J. R. Soc. Interface *5*, 259–271. https://doi.org/10.1098/rsif.2007.1229.

Gu, Y., Han, F., Sainburg, L.E., Schade, M.M., Buxton, O.M., Duyn, J.H., and Liu, X. (2022). An orderly sequence of autonomic and neural events at transient arousal changes. Preprint at bioRxiv. https://doi.org/10.1101/2022.02.05.479238.

Hablitz, L.M., and Nedergaard, M. (2021). The glymphatic system: a novel component of fundamental neurobiology. J. Neurosci. *41*, 7698–7711.

Hablitz, L.M., Vinitsky, H.S., Sun, Q., Stæger, F.F., Sigurdsson, B., Mortensen, K.N., Lilius, T.O., and Nedergaard, M. (2019). Increased glymphatic influx is correlated with high EEG delta power and low heart rate in mice under anesthesia. Sci. Adv. *5*, eaav5447.

Hablitz, L.M., Plá, V., Giannetto, M., Vinitsky, H.S., Stæger, F.F., Metcalfe, T., Nguyen, R., Benrais, A., and Nedergaard, M. (2020). Circadian control of brain glymphatic and lymphatic fluid flow. Nat. Commun. *11*, 4411.

Hadaczek, P., Yamashita, Y., Mirek, H., Tamas, L., Bohn, M.C., Noble, C., Park, J.W., and Bankiewicz, K. (2006). The "perivascular pump" driven by arterial pulsation is a powerful mechanism for the distribution of therapeutic molecules within the brain. Mol. Ther. *14*, 69–78.

Hald, B.O., Jacobsen, J.C.B., Sandow, S.L., Holstein-Rathlou, N.H., and Welsh, D.G. (2014). Less is more: minimal expression of myoendothelial gap junctions optimizes cell-cell communication in virtual arterioles. J. Physiol. *592*, 3243–3255. ISSN 14697793. https://doi.org/10.1113/jphysiol.2014.272815.

Halnes, G., Østby, I., Pettersen, K.H., Omholt, S.W., and Einevoll, G.T. (2013). Electrodiffusive model for astrocytic and neuronal ion concentration dynamics. PLoS Comput. Biol. *9*, e1003386. https://doi.org/10.1371/journal.pcbi.1003386.

Halnes, G., Pettersen, K.H., Øyehaug, L., Rognes, M.E., and Einevoll, G.T. (2019). Astrocytic ion dynamics: implications for potassium buffering and liquid flow. Springer Series in Computational Glioscience *11*, 363. https://doi.org/10.1007/978-3-030-00817-8(14.

Hannocks, M.-J., Pizzo, M.E., Huppert, J., Deshpande, T., Abbott, N.J., Thorne, R.G., and Sorokin, L. (2018). Molecular characterization of perivascular drainage pathways in the murine brain. J. Cereb. Blood Flow Metab. *38*, 669–686.

Hartings, J.A., Shuttleworth, C.W., Kirov, S.A., Ayata, C., Hinzman, J.M., Foreman, B., Andrew, R.D., Boutelle, M.G., Brennan, K.C., Carlson, A.P., et al. (2017). The continuum of spreading depolarizations in acute cortical lesion development: examining Leao's legacy. J. Cereb. Blood Flow Metab. *37*, 1571–1594.

Helakari, H., Korhonen, V., Holst, S.C., Piispala, J., Kallio, M., Väyrynen, T., Huotari, N., Raitamaa, L., Tuunanen, J., Kananen, J., et al. (2022). Human NREM sleep promotes brain-wide vasomotor and respiratory pulsations. J. Neurosci. *42*, 2503–2515.

Hennig, J., Kiviniemi, V., Riemenschneider, B., Barghoorn, A., Akin, B., Wang, F., and LeVan, P. (2020). 15 years MR-encephalography. Magn. Reson. Mater. Phy. *34*, 85–108.

Hladky, S.B., and Barrand, M.A. (2014). Mechanisms of fluid movement into, through and out of the brain: evaluation of the evidence. Fluids Barriers CNS *11*, 26.

Hladky, S.B., and Barrand, M.A. (2018). Elimination of substances from the brain parenchyma: efflux via perivascular pathways and via the blood-brain barrier. Fluids Barriers CNS *15*, 30.

Hladky, S.B., and Barrand, M.A. (2022). The glymphatic hypothesis: the theory and the evidence. Fluids Barriers CNS *19*, 9.

Hov, K.R., Bolstad, N., Idland, A.V., Zetterberg, H., Blennow, K., Chaudhry, F.A., Frihagen, F., Ræder, J., Wyller, T.B., and Watne, L.O. (2017). Cerebrospinal fluid s100b and Alzheimer's disease biomarkers in hip fracture patients with

delirium. Dement. Geriatr. Cogn. Dis. Extra *7*, 374–385.

Hrabe, J., and Hrabetova, S. (2019). Time-resolved integrative optical imaging of diffusion during spreading depression. Biophys. J. *117*, 1783–1794.

Hrabe, J., Hrabetová, S., and Segeth, K. (2004). A model of effective diffusion and tortuosity in the extracellular space of the brain. Biophys. J. *87*, 1606–1617.

Hrabetová, S., Hrabe, J., and Nicholson, C. (2003). Dead-space microdomains hinder extracellular diffusion in rat neocortex during ischemia. J. Neurosci. *23*, 8351–8359.

Hu, D., and Cai, D. (2013). Adaptation and optimization of biological transport networks. Phys. Rev. Lett. *111*, 138701–138705. ISSN 00319007. https://doi.org/10.1103/PhysRevLett.111.138701.

Huang, Y., Potter, R., Sigurdson, W., Santacruz, A., Shih, S., Ju, Y.E., Kasten, T., Morris, J.C., Mintun, M., Duntley, S., et al. (2012). Effects of age and amyloid deposition on a $\beta$ dynamics in the human central nervous system. Arch. Neurol. *69*, 51–58.

Hubbard, J.A., Hsu, M.S., Seldin, M.M., and Binder, D.K. (2015). Expression of the astrocyte water channel aquaporin-4 in the mouse brain. ASN Neuro *7*. 1759091415605486.

Ichimura, T., Fraser, P.A., and Cserr, H.F. (1991). Distribution of extracellular tracers in perivascular spaces of the rat brain. Brain Res. *545*, 103–113.

Idland, A.V., Wyller, T.B., Støen, R., Dahl, G.T., Frihagen, F., Brækhus, A., Hassel, B., and Watne, L.O. (2017). Cerebrospinal fluid phosphate in delirium after hip fracture. Dement. Geriatr. Cogn. Dis. Extra *7*, 309–317.

Iliff, J.J., Wang, M., Liao, Y., Plogg, B.A., Peng, W., Gundersen, G.A., Benveniste, H., Vates, G.E., Deane, R., Goldman, S.A., et al. (2012). A paravascular pathway facilitates CSF flow through the brain parenchyma and the clearance of interstitial solutes, including amyloid beta. Sci. Transl. Med. *4*, 147ra111.

Iliff, J.J., Wang, M., Zeppenfeld, D.M., Venkataraman, A., Plog, B.A., Liao, Y., Deane, R., and Nedergaard, M. (2013a). Cerebral arterial pulsation drives paravascular CSF-interstitial fluid exchange in the murine brain. J. Neurosci. *33*, 18190–18199.

Iliff, J.J., Lee, H., Yu, M., Feng, T., Logan, J., Nedergaard, M., and Benveniste, H. (2013b). Brain-wide pathway for waste clearance captured by contrast-enhanced MRI. J. Clin. Invest. *123*, 1299–1309.

Iliff, J.J., Chen, M.J., Plog, B.A., Zeppenfeld, D.M., Soltero, M., Yang, L., Singh, I., Deane, R., and Nedergaard, M. (2014). Impairment of glymphatic pathway function promotes tau pathology after traumatic brain injury. J. Neurosci. *34*, 16180–16193.

Insel, P.S., Mohlenhoff, B.S., Neylan, T.C., Krystal, A.D., and Scott Mackin, R. (2021). Association of sleep and $\beta$-amyloid pathology among older cognitively unimpaired adults. JAMA Netw. Open *4*, e2117573.

Jacobsen, J.C.B., Mulvany, M.J., and Holstein-Rathlou, N.H. (2008). A mechanism for arteriolar remodeling based on maintenance of smooth muscle cell activation. Am. J. Physiol. Regul. Integr. Comp. Physiol. *294*, R1379–R1389. https://doi.org/10.1152/ajpregu.00407.2007.

Jacobsen, J.C.B., Hornbech, M.S., and Holstein-Rathlou, N.-H. (2009). A tissue in the tissue: models of microvascular plasticity. Eur. J. Pharm. Sci. *36*, 51–61.

Jacobsen, J.C.B., Aalkjaer, C., Nilsson, H., Matchkov, V.V., Freiberg, J., and Holstein-Rathlou, N.-H. (2007). A model of smooth muscle cell synchronization in the arterial wall. Am. J. Physiol. Heart Circ. Physiol. *293*, H229–H237.

Jin, B.J., Smith, A.J., and Verkman, A.S. (2016). Spatial model of convective solute transport in brain extracellular space does not support a "glymphatic" mechanism. J. Gen. Physiol. *148*, 489–501.

Ju, Y.E.S., Ooms, S.J., Sutphen, C., Macauley, S.L., Zangrilli, M.A., Jerome, G., Fagan, A.M., Mignot, E., Zempel, J.M., Claassen, J., and Holtzman, D.M. (2017). Slow wave sleep disruption increases cerebrospinal fluid amyloid-beta levels. Brain *140*, 2104–2111.

Kedarasetti, R.T., Turner, K.L., Echagarruga, C., Gluckman, B.J., Drew, P.J., and Costanzo, F. (2020a). Functional hyperemia drives fluid exchange in the paravascular space. Fluids Barriers CNS *17*, 52.

Kedarasetti, R., Drew, P.J., and Costanzo, F. (2021). Arterial vasodilation drives convective fluid flow in the brain: a poroelastic model. Preprint at bioRxiv. https://doi.org/10.1101/2021.09.23.461603.

Kedarasetti, R.T., Drew, P.J., and Costanzo, F. (2020b). Arterial pulsations drive oscillatory flow of CSF but not directional pumping. Sci. Rep. *10*, 10102.

Holter, K.E., Kehlet, B., Anna, D., Sejnowski, T.J., Dale, A.M., Omholt, S.W., Ottersen, O.P., Nagelhus, E.A., Mardal, K.-A., and Pettersen, K.H. (2017). Interstitial solute transport in 3D reconstructed neuropil occurs by diffusion rather than bulk flow. Proc. Nat. Acad. Sci. USA *114*, 9894–9899.

Keith Sharp, M., Carare, R.O., and Martin, B.A. (2019). Dispersion in porous media in oscillatory flow between flat plates: applications to intrathecal, periarterial and paraarterial solute transport in the central nervous system. Fluids Barriers CNS *16*, 13.

Kevin, T., Mehta, A.I., and Linninger, A.A. (2018). Cerebrospinal fluid dynamics and intrathecal delivery. In Neuromodulation (Elsevier), pp. 829–846.

Kinney, J.P., Spacek, J., Bartol, T.M., Bajaj, C.L., Harris, K.M., and Sejnowski, T.J. (2013). Extracellular sheets and tunnels modulate glutamate diffusion in hippocampal neuropil. J. Comp. Neurol. *521*, 448–464.

Kiviniemi, V., Wang, X., Korhonen, V., Keinänen, T., Tuovinen, T., Autio, J., LeVan, P., Keilholz, S., Zang, Y.-F., Hennig, J., and Nedergaard, M. (2016). Ultra-fast magnetic resonance encephalography of physiological brain activity–glymphatic pulsation mechanisms? J. Cereb. Blood Flow Metab. *36*, 1033–1045.

Korogod, N., Petersen, C.C., and Knott, G.W. (2015). Ultrastructural analysis of adult mouse neocortex comparing aldehyde perfusion with cryo fixation. Elife *4*, e5793.

Koundal, S., Elkin, R., Nadeem, S., Xue, Y., Constantinou, S., Sanggaard, S., Liu, X., Monte, B., Xu, F., Van Nostrand, W., et al. (2020). Optimal mass transport with Lagrangian workflow reveals advective and diffusion driven solute transport in the glymphatic system. Sci. Rep. *10*, 1990.

Kovacech, B., and Novak, M. (2010). Tau truncation is a productive posttranslational modification of neurofibrillary degeneration in Alzheimer's disease. Curr. Alzheimer Res. *7*, 708–716.

Kress, B.T., Iliff, J.J., Xia, M., Wang, M., Wei, H.S., Zeppenfeld, D., Xie, L., Kang, H., Xu, Q., Liew, J.A., et al. (2014). Impairment of paravascular clearance pathways in the aging brain. Ann. Neurol. *76*, 845–861.

Kurth, S., Riedner, B.A., Dean, D.C., O'Muircheartaigh, J., Huber, R., Jenni, O.G., Deoni, S.C.L., and LeBourgeois, M.K. (2017). Traveling slow oscillations during sleep: a marker of brain connectivity in childhood. Sleep *40*, 07.

Ladrón-de Guevara, A., Shang, J.K., Nedergaard, M., and Kelley, D.H. (2020). Perivascular pumping in the mouse brain: realistic boundary conditions reconcile theory, simulation, and experiment. Preprint at bioRxiv. https://doi.org/10.1101/2020.07.02.183608.

Lauritzen, M., and Strong, A.J. (2017). Strong. 'spreading depression of leão'and its emerging relevance to acute brain injury in humans. J. Cereb. Blood Flow Metab. *37*, 1553–1570.

Lee, H., Xie, L., Yu, M., Kang, H., Feng, T., Deane, R., Logan, J., Nedergaard, M., and Benveniste, H. (2015). The effect of body posture on brain glymphatic transport. J. Neurosci. *35*, 11034–11044. https://doi.org/10.1523/JNEUROSCI.1625-15.2015.

Lee, H., Mortensen, K., Sanggaard, S., Koch, P., Brunner, H., Quistorff, B., Nedergaard, M., and Benveniste, H. (2018). Quantitative Gd-DOTA uptake from cerebrospinal fluid into rat brain using 3D VFA-SPGR at 9.4T. Magn. Reson. Med. *79*, 1568–1578. https://doi.org/10.1002/mrm.26779.

Levin, V.A., Fenstermacher, J.D., and Patlak, C.S. (1970). Sucrose and inulin space measurements of cerebral cortex in four mammalian species. Am. J. Physiol. *219*, 1528–1533.

Lilius, T.O., Blomqvist, K., Hauglund, N.L., Liu, G., Stæger, F.F., Bærentzen, S., Du, T., Ahlström, F., Backman, J.T., Kalso, E.A., et al. (2019). Dexmedetomidine enhances glymphatic brain delivery of intrathecally administered drugs. J. Control. Release *304*, 29–38. https://doi.org/10.1016/j.jconrel.2019.05.005.

Linninger, A.A., Somayaji, M.R., Mekarski, M., and Zhang, L. (2008). Prediction of convection-enhanced drug delivery to the human brain. J. Theor. Biol. *250*, 125–138.

Linninger, A.A., Xu, C., Tangen, K., and Hartung, G. (2017). Starling forces drive intracranial water exchange during normal and pathological states. Croat. Med. J. *58*, 384–394.

Linninger, A.A., Xenos, M., Sweetman, B., Ponkshe, S., Guo, X., and Penn, R. (2009). A mathematical model of blood, cerebrospinal fluid and brain dynamics. J. Math. Biol. *59*, 729–759.

Linninger, A.A., Tangen, K., Hsu, C.-Y., and Frim, D. (2016). Cerebrospinal fluid mechanics and its coupling to cerebrovascular dynamics. Annu. Rev. Fluid Mech. *48*, 219–257.

Liu, G., Mestre, H., Sweeney, A.M., Sun, Q., Weikop, P., Du, T., and Nedergaard, M. (2020). Direct measurement of cerebrospinal fluid production in mice. Cell Rep. *33*, 108524.

Louveau, A., Smirnov, I., Keyes, T.J., Eccles, J.D., Rouhani, S.J., Peske, J.D., Derecki, N.C., Castle, D., Mandell, J.W., Lee, K.S., et al. (2015). Structural and functional features of central nervous system lymphatic vessels. Nature *523*, 337–341. https://doi.org/10.1038/nature14432.

Lundgaard, I., Lu, M.L., Yang, E., Peng, W., Mestre, H., Hitomi, E., Deane, R., and Nedergaard, M. (2017). Glymphatic clearance controls state-dependent changes in brain lactate concentration. J. Cereb. Blood Flow Metab. *37*, 2112–2124.

Ma, Q., Ineichen, B.V., Detmar, M., and Proulx, S.T. (2017). Outflow of cerebrospinal fluid is predominantly through lymphatic vessels and is reduced in aged mice. Nat. Commun. *8*, 1434.

Magdoom, K.N., Brown, A., Rey, J., Mareci, T.H., King, M.A., and Sarntinoranont, M. (2019). Mri of whole rat brain perivascular network reveals role for ventricles in brain waste clearance. Sci. Rep. *9*, 11480.

Margaris, K.N., and Black, R.A. (2012). Modelling the lymphatic system: challenges and opportunities. J. R. Soc. Interface *9*, 601–612.

Martens, E.A., and Klemm, K. (2017). Transitions from trees to cycles in adaptive flow networks. Front. Phys. *5*, 1–10. https://doi.org/10.3389/fphy.2017.00062.

Martinac, A.D., and Bilston, L.E. (2019). Computational modelling of fluid and solute transport in the brain. Biomech. Model. Mechanobiol. *19*, 781–800.

Martinac, A.D., Fletcher, D.F., and Bilston, L.E. (2021). Phase offset between arterial pulsations and subarachnoid space pressure fluctuations are unlikely to drive periarterial cerebrospinal fluid flow. Biomech. Model. Mechanobiol. *20*, 1751–1766.

Massimini, M., Huber, R., Ferrarelli, F., Hill, S., and Tononi, G. (2004). The sleep slow oscillation as a traveling wave. J. Neurosci. *24*, 6862–6870. https://doi.org/10.1523/JNEUROSCI.1318-04.2004.

Mestre, H., Tithof, J., Du, T., Song, W., Peng, W., Sweeney, A.M., Olveda, G., Thomas, J.H., Nedergaard, M., and Kelley, D.H. (2018a). Flow of cerebrospinal fluid is driven by arterial pulsations and is reduced in hypertension. Nat. Commun. *9*, 4878.

Mestre, H., Hablitz, L.M., Xavier, A.L., Feng, W., Zou, W., Pu, T., Monai, H., Murlidharan, G., Castellanos Rivera, R.M., Simon, M.J., et al. (2018b). Aquaporin-4-dependent glymphatic solute transport in the rodent brain. Elife *7*, e40070. https://doi.org/10.7554/eLife.40070.

Mestre, H., Du, T., Sweeney, A.M., Liu, G., Samson, A.J., Peng, W., Kristian, N.M., Frederik, F.S., Stæger, F.F., Bork, P.A.R., et al. (2020a). Cerebrospinal fluid influx drives acute ischemic tissue swelling. Science *367*, eaax7171–eaax7224.

Mestre, H., Mori, Y., and Nedergaard, M. (2020b). The brain's glymphatic system: current controversies. Trends Neurosci. *43*, 458–466.

Min Rivas, F., Liu, J., Martell, B.C., Du, T., Mestre, H., Nedergaard, M., Tithof, J., Thomas, J.H., and Kelley, D.H. (2020). Surface periarterial spaces of the mouse brain are open, not porous. J. R. Soc. Interface *17*, 20200593.

Monai, H., Wang, X., Yahagi, K., Lou, N., Mestre, H., Xu, Q., Abe, Y., Yasui, M., Iwai, Y., Nedergaard, M., and Hirase, H. (2019). Adrenergic receptor antagonism induces neuroprotection and facilitates recovery from acute ischemic stroke. Proc. Natl. Acad. Sci. USA *116*, 11010–11019. https://doi.org/10.1073/pnas.1817347116.

Moore, J.E., Jr., and Bertram, C.D. (2018). Lymphatic system flows. Annu. Rev. Fluid Mech. *50*, 459–482.

Morawska, M.M., Moreira, C.G., Ginde, V.R., Valko, P.O., Weiss, T., Büchele, F., Imbach, L.L., Masneuf, S., Kollarik, S., Prymaczok, N., et al. (2021). Slow-wave sleep affects synucleinopathy and regulates proteostatic processes in mouse models of Parkinson's disease. Sci. Transl. Med. *13*, eabe7099. https://doi.org/10.1126/scitranslmed.abe7099.

Mortensen, K.N., Sanggaard, S., Mestre, H., Lee, H., Kostrikov, S., Xavier, A.L.R., Gjedde, A., Benveniste, H., and Nedergaard, M. (2019). Impaired glymphatic transport in spontaneously hypertensive rats. J. Neurosci. *39*, 6365–6377. https://doi.org/10.1523/JNEUROSCI.1974-18.2019.

Nagelhus, E.A., Veruki, M.L., Torp, R., Haug, F.M., Laake, J.H., Nielsen, S., Agre, P., and Ottersen, O.P. (1998). Aquaporin-4 water channel protein in the rat retina and optic nerve: polarized expression in Müller cells and fibrous astrocytes. J. Neurosci. *18*, 2506–2519.

Nägerl, U.V., Willig, K.I., Hein, B., Hell, S.W., and Bonhoeffer, T. (2008). Live-cell imaging of dendritic spines by sted microscopy. Proc. Natl. Acad. Sci. USA *105*, 18982–18987. https://doi.org/10.1073/pnas.0810028105.

Nakamura, K., Brown, R.A., Narayanan, S., Collins, D.L., and Arnold, D.L.; Alzheimer's Disease Neuroimaging Initiative (2015). Diurnal fluctuations in brain volume: statistical analyses of MRI from large populations. Neuroimage *118*, 126–132. https://doi.org/10.1016/j.neuroimage.2015.05.077.

Nedergaard, M., and Goldman, S.A. (2020). Glymphatic failure as a final common pathway to dementia. Science *370*, 50–56. https://doi.org/10.1126/science.abb8739.

Nedergaard, M. (2013). Garbage truck of the brain. Science *340*, 1529–1530. https://doi.org/10.1126/science.1240514.

Nicholson, C., and Hrabětová, S. (2017). Brain extracellular space: the final Frontier of neuroscience. Biophys. J. *113*, 2133–2142.

Nicholson, C., and Kamali-Zare, P. (2020). Reduction of dimensionality in Monte Carlo simulation of diffusion in extracellular space surrounding cubic cells. Neurochem. Res. *45*, 42–52.

Nicholson, C., and Phillips, J.M. (1981). Ion diffusion modified by tortuosity and volume fraction in the extracellular microenvironment of the rat cerebellum. J. Physiol. *321*, 225–257.

Nicholson, C., and Tao, L. (1993). Hindered diffusion of high molecular weight compounds in brain extracellular microenvironment measured with integrative optical imaging. Biophys. J. *65*, 2277–2290.

Nicholson, C. (2018). Brain interstitial structure revealed through diffusive spread of molecules. In Diffusive Spreading in Nature, Technology and Society (Springer), pp. 93–114.

Nicholson, C. (1992). Quantitative analysis of extracellular space using the method of TMA+ iontophoresis and the issue of TMA+ uptake. Can. J. Physiol. Pharmacol. *70*, S314–S322.

Nielsen, S., Nagelhus, E.A., Amiry-Moghaddam, M., Bourque, C., Agre, P., and Ottersen, O.P. (1997). Specialized membrane domains for water transport in glial cells: high-resolution immunogold cytochemistry of aquaporin-4 in rat brain. J. Neurosci. *17*, 171–180.

Ooms, S., Overeem, S., Besse, K., Rikkert, M.O., Verbeek, M., and Claassen, J.A.H.R. (2014). Effect of 1 night of total sleep deprivation on cerebrospinal fluid beta-amyloid 42 in healthy middle-aged men: a randomized clinical trial. JAMA Neurol. *71*, 971–977. https://doi.org/10.1001/jamaneurol.2014.1173.

Ozturk, B.O., Monte, B., Koundal, S., Dai, F., Benveniste, H., and Lee, H. (2021). Disparate volumetric fluid shifts across cerebral tissue compartments with two different anesthetics. Fluids Barriers CNS *18*, 1.

Patel, T.K., Habimana-Griffin, L., Gao, X., Xu, B., Achilefu, S., Alitalo, K., McKee, C.A., Sheehan, P.W., Musiek, E.S., Xiong, C., et al. (2019). Dural lymphatics regulate clearance of extracellular tau from the CNS. Mol. Neurodegener. *14*, 11. https://doi.org/10.1186/s13024-019-0312-x.

Patterson, B.W., Elbert, D.L., Mawuenyega, K.G., Kasten, T., Ovod, V., Ma, S., Xiong, C., Chott, R., Yarasheski, K., Sigurdson, W., et al. (2015). Age and amyloid effects on human central nervous system amyloid-beta kinetics. Ann. Neurol. *78*, 439–453. https://doi.org/10.1002/ana.24454.

Paviolo, C., Soria, F.N., Ferreira, J.S., Lee, A., Groc, L., Bezard, E., and Cognet, L. (2020). Nanoscale exploration of the extracellular space in the live brain by combining single carbon nanotube tracking and super-resolution imaging analysis. Methods *2020*, 91–99.

Petitclerc, L., Hirschler, L., Wells, J.A., Thomas, D.L., van Walderveen, M.A.A., van Buchem, M.A.,

van Osch, M.J.P., and Matthias, J.P. (2021). Ultra-long-TE arterial spin labeling reveals rapid and brain-wide blood-to-CSF water transport in humans. Neuroimage *245*, 118755. https://doi.org/10.1016/j.neuroimage.2021.118755.

Phillips, J.M., and Nicholson, C. (1979). Anion permeability in spreading depression investigated with ion-sensitive microelectrodes. Brain Res. *173*, 567–571.

Plog, B.A., Dashnaw, M.L., Hitomi, E., Peng, W., Liao, Y., Lou, N., Deane, R., and Nedergaard, M. (2015). Biomarkers of traumatic injury are transported from brain to blood via the glymphatic system. J. Neurosci. *35*, 518–526.

Plog, B.A., Mestre, H., Olveda, G.E., Sweeney, A.M., Kenney, H.M., Cove, A., Dholakia, K.Y., Tithof, J., Nevins, T.D., Lundgaard, I., et al. (2018). Transcranial optical imaging reveals a pathway for optimizing the delivery of immunotherapeutics to the brain. JCI Insight *3*, 126138. https://doi.org/10.1172/jci.insight.126138.

Plog, B.A., Lou, N., Pierre, C.A., Cove, A., Kenney, H.M., Hitomi, E., Kang, H., Iliff, J.J., Zeppenfeld, D.M., Nedergaard, M., and Vates, G.E. (2020). When the air hits your brain: decreased arterial pulsatility after craniectomy leading to impaired glymphatic flow. J. Neurosurg. *133*, 210–223. https://doi.org/10.3171/2019.2.JNS182675.

Polimeni, J.R., and Lewis, L.D. (2021). Imaging faster neural dynamics with fast fMRI: a need for updated models of the hemodynamic response. Prog. Neurobiol. *207*, 102174.

Porter, M.A., and Gleeson, J.P. (2016). In Dynamical Systems on Networks, *volume* 4Dynamical Systems on Networks (Springer). https://doi.org/10.4171/JEMS/577.

Posse, S., Ackley, E., Mutihac, R., Zhang, T., Hummatov, R., Akhtari, M., Chohan, M., Fisch, B., and Yonas, H. (2013). High-speed real-time resting-state FMRI using multi-slab echo-volumar imaging. Front. Hum. Neurosci. *7*, 479.

Raghunandan, A., Ladron-de Guevara, A., Tithof, J., Mestre, H., Du, T., Nedergaard, M., Thomas, J.H., and Kelley, D.H. (2021). Bulk flow of cerebrospinal fluid observed in periarterial spaces is not an artifact of injection. Elife *10*, e65958. https://doi.org/10.7554/eLife.65958.

Raitamaa, L., Huotari, N., Korhonen, V., Helakari, H., Koivula, A., Kananen, J., and Kiviniemi, V. (2021). Spectral analysis of physiological brain pulsations affecting the bold signal. Hum. Brain Mapp. *42*, 4298–4313.

Rajna, Z., Mattila, H., Huotari, N., Tuovinen, T., Krüger, J., Holst, S.C., Korhonen, V., Remes, A.M., Seppänen, T., Hennig, J., et al. (2021). Cardiovascular brain impulses in Alzheimer's disease. Brain *144*, 2214–2226.

Rasmussen, M.K., Mestre, H., and Nedergaard, M. (2018). The glymphatic pathway in neurological disorders. Lancet Neurol. *17*, 1016–1024.

Rasmussen, M.K., Mestre, H., and Nedergaard, M. (2021). Fluid transport in the brain. Physiol. Rev. *102*, 1025–1151. https://doi.org/10.1152/physrev.00031.2020.

Ray, L.A., and Heys, J.J. (2019). Fluid flow and mass transport in brain tissue. Fluids *4*, 196–233.

Ray, L., Iliff, J.J., and Heys, J.J. (2019). Analysis of convective and diffusive transport in the brain interstitium. Fluids Barriers CNS *16*, 6–18.

Ray, L.A., Pike, M., Simon, M., Iliff, J.J., and Heys, J.J. (2021). Quantitative analysis of macroscopic solute transport in the murine brain. Fluids Barriers CNS *18*, 55.

Rennels, M.L., Gregory, T.F., Blaumanis, O.R., Fujimoto, K., and Grady, P.A. (1985). Evidence for a 'paravascular' fluid circulation in the mammalian central nervous system, provided by the rapid distribution of tracer protein throughout the brain from the subarachnoid space. Brain Res. *326*, 47–63.

Rennels, M.L., Blaumanis, O.R., and Grady, P.A. (1990). Rapid solute transport throughout the brain via paravascular fluid pathways. Adv. Neurol. *52*, 431–439.

Rey, J., and Sarntinoranont, M. (2018). Pulsatile flow drivers in brain parenchyma and perivascular spaces: a resistance network model study. Fluids Barriers CNS *15*, 20.

Ringstad, G., and Eide, P.K. (2020). Cerebrospinal fluid tracer efflux to parasagittal dura in humans. Nat. Commun. *11*, 354. https://doi.org/10.1038/s41467-019-14195-x.

Ringstad, G., Vatnehol, S.A.S., and Eide, P.K. (2017). Glymphatic MRI in idiopathic normal pressure hydrocephalus. Brain *140*, 2691–2705. https://doi.org/10.1093/brain/awx191.

Ringstad, G., Valnes, L.M., Dale, A.M., Pripp, A.H., Vatnehol, S.A.S., Emblem, K.E., Mardal, K.A., and Eide, P.K. (2018). Brain-Wide glymphatic enhancement and clearance in humans assessed with MRI. JCI insight *3*, 121537.

Romanò, F., Suresh, V., Galie, P.A., and Grotberg, J.B. (2020). Peristaltic flow in the glymphatic system. Sci. Rep. *10*, 21065.

Rosenberg, G.A., Kyner, W.T., and Estrada, E. (1980). Bulk flow of brain interstitial fluid under normal and hyperosmolar conditions. Am. J. Physiol. *238*, F42–F49.

Rungta, R.L., Chaigneau, E., Osmanski, B.F., and Charpak, S. (2018). Vascular compartmentalization of functional hyperemia from the synapse to the pia. Neuron *99*, 362–375.e4.

Rustenhoven, J., Drieu, A., Mamuladze, T., de Lima, K.A., Dykstra, T., Wall, M., Papadopoulos, Z., Kanamori, M., Salvador, A.F., Baker, W., et al. (2021). Functional characterization of the dural sinuses as a neuroimmune interface. Cell *184*, 1000–1016.e27. https://doi.org/10.1016/j.cell.2020.12.040.

Santisakultarm, T.P., Cornelius, N.R., Nishimura, N., Schafer, A.I., Silver, R.T., Doerschuk, P.C., Olbricht, W.L., and Schaffer, C.B. (2012). In vivo two-photon excited fluorescence microscopy reveals cardiac-and respiration-dependent pulsatile blood flow in cortical blood vessels in mice. Am. J. Physiol. Heart Circ. Physiol. *302*, H1367–H1377.

Sato, C., Barthélemy, N.R., Mawuenyega, K.G., Patterson, B.W., Gordon, B.A., Jockel-Balsarotti, J., Sullivan, M., Crisp, M.J., Kasten, T., Kirmess, K.M., et al. (2018). Tau kinetics in neurons and the human central nervous system. Neuron *98*, 861–864. https://doi.org/10.1016/j.neuron.2018.04.035.

Schain, A.J., Melo-Carrillo, A., Strassman, A.M., and Burstein, R. (2017). Cortical spreading depression closes paravascular space and impairs glymphatic flow: implications for migraine headache. J. Neurosci. *37*, 2904–2915.

Schley, D., Carare-Nnadi, R., Please, C.P., Perry, V.H., and Weller, R.O. (2006). Mechanisms to explain the reverse perivascular transport of solutes out of the brain. J. Theor. Biol. *238*, 962–974.

Schreder, H.E., Liu, J., Kelley, D.H., Thomas, J.H., and Boster, K.A.S. (2022). A hydraulic resistance model for interstitial fluid flow in the brain. J. R. Soc. Interface *19*, 20210812.

Schulz, A., Ajayi, T., Specchio, N., de Los Reyes, E., Gissen, P., Ballon, D., Dyke, J.P., Cahan, H., Slasor, P., Jacoby, D., and Kohlschütter, A. (2018). Study of intraventricular cerliponase alfa for CLN2 disease. N. Engl. J. Med. Overseas. Ed. *378*, 1898–1907.

Selkoe, D.J., and Hardy, J. (2016). The amyloid hypothesis of alzheimer's disease at 25 years. EMBO Mol. Med. *8*, 595–608. https://doi.org/10.15252/emmm.201606210.

Shokri-Kojori, E., Wang, G.J., Wiers, C.E., Demiral, S.B., Guo, M., Kim, S.W., Lindgren, E., Ramirez, V., Zehra, A., Freeman, C., et al. (2018). $\beta$ Amyloid accumulation in the human brain after one night of sleep deprivation. Proc. Natl. Acad. Sci. USA *115*, 4483–4488.

Sloots, J.J., Biessels, G.J., and Zwanenburg, J.J.M. (2020). Cardiac and respiration-induced brain deformations in humans quantified with high-field MRI. Neuroimage *210*, 116581.

Smith, A.J., and Verkman, A.S. (2018). The "glymphatic" mechanism for solute clearance in Alzheimer's disease: game changer or unproven speculation? Faseb. J. *32*, 543–551.

Smith, A.J., Yao, X., Dix, J.A., Jin, B.J., and Verkman, A.S. (2017). Test of the 'glymphatic' hypothesis demonstrates diffusive and aquaporin-4-independent solute transport in rodent brain parenchyma. Elife *6*, e27679. https://doi.org/10.7554/elife.27679.

Soltoff-Schiller, B., Goldfischer, S., Adamany, A.M., and Wolinsky, H. (1976). Endocytosis by vascular smooth muscle cells in vivo and in vitro. roles or vesicles and lysosomes. Am. J. Pathol. *83*, 45–60.

Somjen, G.G. (2001). Mechanisms of spreading depression and hypoxic spreading depression-like depolarization. Physiol. Rev. *81*, 1065–1096.

Soria, F.N., Miguelez, C., Peñagarikano, O., and Tønnesen, J. (2020). Current techniques for investigating the brain extracellular space. Front. Neurosci. *14*, 570750.

Spira, A.P., Gamaldo, A.A., An, Y., Wu, M.N., Simonsick, E.M., Bilgel, M., Zhou, Y., Wong, D.F., Ferrucci, L., and Resnick, S.M. (2013).

Self-reported sleep and beta-amyloid deposition in community-dwelling older adults. JAMA Neurol. *70*, 1537–1543. https://doi.org/10.1001/jamaneurol.2013.4258.

Staats, P.S., Yearwood, T., Charapata, S.G., Presley, R.W., Wallace, M.S., Byas-Smith, M., Fisher, R., Bryce, D.A., Mangieri, E.A., Luther, R.R., et al. (2004). Intrathecal ziconotide in the treatment of refractory pain in patients with cancer or AIDS: a randomized controlled trial. JAMA *291*, 63–70.

Stanton, E.H., Persson, N.D.Å., Gomolka, R.S., Lilius, T., Sigurðsson, B., Lee, H., Xavier, A.L.R., Benveniste, H., Nedergaard, M., and Mori, Y. (2021). Mapping of CSF transport using high spatiotemporal resolution dynamic contrast-enhanced MRI in mice: effect of anesthesia. Magn. Reson. Med. *85*, 3326–3342. https://doi.org/10.1002/mrm.28645.

Steven, T.P. (2021). Cerebrospinal fluid outflow: a review of the historical and contemporary evidence for arachnoid villi, perineural routes, and dural lymphatics. Cell. Mol. Life Sci. *78*, 2429–2457.

Sun, Y., and Sun, X. (2021). Exploring the interstitial system in the brain: the last mile of drug delivery. Rev. Neurosci. *32*, 363–377.

Syková, E., and Nicholson, C. (2008). Diffusion in brain extracellular space. Physiol. Rev. *88*, 1277–1340. https://doi.org/10.1152/physrev.00027.2007.

Tangen, K.M., Leval, R., Mehta, A.I., and Linninger, A.A. (2017). Computational and in vitro experimental investigation of intrathecal drug distribution: parametric study of the effect of injection volume, cerebrospinal fluid pulsatility, and drug uptake. Anesth. Analg. *124*, 1686–1696.

Tangen, K., Nestorov, I., Verma, A., Sullivan, J., Holt, R.W., and Linninger, A.A. (2020). In vivo intrathecal tracer dispersion in cynomolgus monkey validates wide biodistribution along neuraxis. IEEE Trans. Biomed. Eng. *67*, 1122–1132.

Tao, L., and Nicholson, C. (2004). Maximum geometrical hindrance to diffusion in brain extracellular space surrounding uniformly spaced convex cells. J. Theor. Biol. *229*, 59–68.

Tao, A., Tao, L., and Nicholson, C. (2005). Cell cavities increase tortuosity in brain extracellular space. J. Theor. Biol. *234*, 525–536.

Tarasoff-Conway, J.M., Carare, R.O., Osorio, R.S., Glodzik, L., Butler, T., Fieremans, E., Axel, L., Rusinek, H., Nicholson, C., Zlokovic, B.V., et al. (2016). Clearance systems in the brain–implications for Alzheimer disease. Nat. Rev. Neurol. *12*, 248. https://doi.org/10.1038/nrneurol.2016.36.

Terstappen, G.C., Meyer, A.H., Bell, R.D., and Zhang, W. (2021). Strategies for delivering therapeutics across the blood–brain barrier. Nat. Rev. Drug Discov. *20*, 362–383.

Thal, D.R., Ghebremedhin, E., Rüb, U., Yamaguchi, H., Del Tredici, K., and Braak, H. (2002). Two types of sporadic cerebral amyloid angiopathy. J. Neuropathol. Exp. Neurol. *61*, 282–293.

Thomas, J.H. (2019). Fluid dynamics of cerebrospinal fluid flow in perivascular spaces. J. R. Soc. Interface *16*, 20190572. https://doi.org/10.1098/rsif.2019.0572.

Thomas, J.H. (2022). Theoretical analysis of wake/sleep changes in brain solute transport suggests a flow of interstitial fluid. Fluids Barriers CNS *19*, 30.

Thorne, R.G., and Nicholson, C. (2006). In vivo diffusion analysis with quantum dots and dextrans predicts the width of brain extracellular space. Proc. Natl. Acad. Sci. USA *103*, 5567–5572.

Tian, P., Teng, I.C., May, L.D., Kurz, R., Lu, K., Scadeng, M., Hillman, E.M.C., De Crespigny, A.J., D'Arceuil, H.E., Mandeville, J.B., et al. (2010). Cortical depth-specific microvascular dilation underlies laminar differences in blood oxygenation level-dependent functional mri signal. Proc. Natl. Acad. Sci. USA *107*, 15246–15251.

Tithof, J., Kelley, D.H., Mestre, H., Nedergaard, M., and Thomas, J.H. (2019). Hydraulic resistance of periarterial spaces in the brain. Fluids Barriers CNS *16*, 19.

Tithof, J., Boster, K.A.S., Bork, P.A.R., Nedergaard, M., Thomas, J.H., Kelley, D.H., and Kelley, D.H. (2022). A network model of glymphatic flow under different experimentally-motivated parametric scenarios. iScience *25*, 104258.

Tønnesen, J., Inavalli, V.V.G.K., and Nägerl, U.V. (2018). Super-resolution imaging of the extracellular space in living brain tissue. Cell *172*, 1108–1121.e15.

Troyetsky, D.E., Tithof, J., Thomas, J.H., and Kelley, D.H. (2021). Dispersion as a waste-clearance mechanism in flow through penetrating perivascular spaces in the brain. Sci. Rep. *11*, 4595.

Tuovinen, T., Kananen, J., Rajna, Z., Lieslehto, J., Korhonen, V., Rytty, R., Mattila, H., Huotari, N., Raitamaa, L., Helakari, H., et al. (2020). The variability of functional MRI brain signal increases in Alzheimer's disease at cardiorespiratory frequencies. Sci. Rep. *10*, 21559–21611.

Turner, K.L., Gheres, K.W., Proctor, E.A., and Drew, P.J. (2020). Neurovascular coupling and bilateral connectivity during NREM and REM sleep. Elife, e62071.

Valnes, L.M., Mitusch, S.K., Ringstad, G., Eide, P.K., Funke, S.W., and Mardal, K.A. (2020). Apparent diffusion coefficient estimates based on 24 hours tracer movement support glymphatic transport in human cerebral cortex. Sci. Rep. *10*, 9176. https://doi.org/10.1038/s41598-020-66042-5.

Van Harreveld, A., and Khattab, F.I. (1967). Changes in cortical extracellular space during spreading depression investigated with the electron microscope. J. Neurophysiol. *30*, 911–929.

van Veluw, S.J., Hou, S.S., Calvo-Rodriguez, M., Arbel-Ornath, M., Snyder, A.C., Frosch, M.P., Greenberg, S.M., and Bacskai, B.J. (2020). Vasomotion as a driving force for paravascular clearance in the awake mouse brain. Neuron *105*, 549–561.e5.

Vardakis, J.C., Chou, D., Guo, L., and Ventikos, Y. (2020). Exploring neurodegenerative disorders using a novel integrated model of cerebral transport: initial results. Proc. Inst. Mech. Eng. H *234*, 1223–1234.

Venugopal, I., Habib, N., and Linninger, A. (2017). Intrathecal magnetic drug targeting for localized delivery of therapeutics in the CNS. Nanomedicine *12*, 865–877.

Verma, A., Hesterman, J.Y., Chazen, J.L., Holt, R., Connolly, P., Horky, L., Vallabhajosula, S., and Mozley, P.D. (2020). Intrathecal 99mTc-DTPA imaging of molecular passage from lumbar cerebrospinal fluid to brain and periphery in humans. Alzheimers Dement. *12*, e12030.

Vinje, V., Ringstad, G., Lindstrøm, E.K., Valnes, L.M., Rognes, M.E., Eide, P.K., and Mardal, K.-A. (2019). Respiratory influence on cerebrospinal fluid flow–a computational study based on long-term intracranial pressure measurements. Sci. Rep. *9*, 9732–9813.

Vinje, V., Eklund, A., Mardal, K.-A., Rognes, M.E., and Støverud, K.H. (2020). Intracranial pressure elevation alters CSF clearance pathways. Fluids Barriers CNS *17*, 29.

Vinje, V., Bakker, E.N.T.P., and Rognes, M.E. (2021). Brain solute transport is more rapid in periarterial than perivenous spaces. Sci. Rep. *11*, 16085.

Vyazovskiy, V.V., and Harris, K.D. (2013). Sleep and the single neuron: the role of global slow oscillations in individual cell rest. Nat. Rev. Neurosci. *14*, 443–451.

Wang, P., and Olbricht, W.L. (2011). Fluid mechanics in the perivascular space. J. Theor. Biol. *274*, 52–57.

Wang, M.X., Ray, L., Tanaka, K.F., Iliff, J.J., and Heys, J. (2021). Varying perivascular astroglial endfoot dimensions along the vascular tree maintain perivascular-interstitial flux through the cortical mantle. Glia *69*, 715–728.

Wardlaw, J.M., Benveniste, H., Nedergaard, M., Zlokovic, B.V., Mestre, H., Lee, H., Doubal, F.N., Brown, R., Ramirez, J., MacIntosh, B.J., et al. (2020). Perivascular spaces in the brain: anatomy, physiology and pathology. Nat. Rev. Neurol. *16*, 137–153. https://doi.org/10.1038/s41582-020-0312-z.

Waters, J. (2011). The concentration of soluble extracellular amyloid-$\beta$ protein in acute brain slices from CRND8 mice. PLoS One *5*, 1–16. https://doi.org/10.1371/journal.pone.0015709.

Wen, S.W., and Wong, C.H.Y. (2019). Aging- and vascular-related pathologies. Microcirculation *26*, e12463. https://doi.org/10.1111/micc.12463.

West, G.B., Brown, J.H., and Enquist, B.J. (1997). A general model for the origin of allometric scaling laws in biology. Science *276*, 122–126.

Wigner, E.P. (1990). The unreasonable effectiveness of mathematics in the natural sciences. In Mathematics and science (World Scientific), pp. 291–306.

Wiig, H., and Swartz, M.A. (2012). Interstitial fluid and lymph formation and transport: physiological

regulation and roles in inflammation and cancer. Physiol. Rev. *92*, 1005–1060. https://doi.org/10.1152/physrev.00037.2011.

Winer, J.R., Allison, M., Fenton, L., Harrison, T.M., Ayangma, L., Reed, M., Kumar, S., Suzanne, L., Baker, W.J.J., and Walker, M.P. (2021). Tau and $\beta$-amyloid burden predict actigraphy-measured and self-reported impairment and misperception of human sleep. J. Neurosci. *41*, 7687–7696. https://doi.org/10.1523/JNEUROSCI.0353-21.2021.

Wolak, D.J., and Thorne, R.G. (2013). Diffusion of macromolecules in the brain: implications for drug delivery. Mol. Pharm. *10*, 1492–1504.

Sherpa, A.D., Xiao, F., Joseph, N., Aoki, C., and Hrabetova, S. (2016). Activation of $\beta$-adrenergic receptors in rat visual cortex expands astrocytic processes and reduces extracellular space volume. Synapse *70*, 307–316.

Xie, L., Kang, H., Xu, Q., Chen, M.J., Liao, Y., Thiyagarajan, M., O'Donnell, J., Christensen, D.J., Nicholson, C., Iliff, J.J., et al. (2013). Sleep drives metabolite clearance from the adult brain. Science *342*, 373–377. https://doi.org/10.1126/science.1241224.

Yokoyama, N., Takeishi, N., and Wada, S. (2021). Cerebrospinal fluid flow driven by arterial pulsations in axisymmetric perivascular spaces: analogy with Taylor's swimming sheet. J. Theor. Biol. *523*, 110709.

Young, B.A., Adams, J., Beary, J.M., Mardal, K.A., Schneider, R., and Kondrashova, T. (2021). Kent-andre mardal, robert schneider, and tatyana kondrashova. Variations in the cerebrospinal fluid dynamics of the american alligator (alligator mississippiensis). Fluids Barriers CNS *18*, 11.

Zheng, K., Jensen, T.P., Savtchenko, L.P., Levitt, J.A., Suhling, K., and Rusakov, D.A. (2017). Nanoscale diffusion in the synaptic cleft and beyond measured with time-resolved fluorescence anisotropy imaging. Sci. Rep. *7*, 42022–42110.